Equation of state for supernovae and neutron stars

H. Shen — *Nankai University, Tianjin, China*

申虹 — 南開大学 天津 中国

In collaboration with

H. Toki — *RCNP, Osaka University, Japan*

K. Sumiyoshi — *Numazu College of Technology, Japan*

K. Oyamatsu — *Aichi Shukutoku University, Japan*

J. N. Hu — *Nankai University, Tianjin, China*

Z. W. Zhang — *Shanghai Jiao Tong University, China*

S. S. Bao — *Nankai University, Tianjin, China*

X. H. Wu — *Nankai University, Tianjin, China*

Contents

- Introduction
- EOS tables for supernovae
- Developments of EOS tables
- Symmetry energy effects
- Summary

Introduction

nuclear physics

astrophysics

unstable nuclei

equation of state

- supernova explosion
- proton-neutron star cooling
- neutron star properties
- ⋮

Classification of EOS's

neutron star matter: charge neutrality; β equilibrium; $T\sim 0$

supernova matter: charge neutrality; fixed fractions; $T\neq 0$

EOS for supernovae

single nucleus approximation (SNA)

J. M. Lattimer and F. D. Swesty, Nucl. Phys. A 535, 331 (1991)

liquid-drop model with Skyrme force

H. Shen, H. Toki, K. Oyamatsu, K. Sumiyoshi, Prog. Theor. Phys. 100, 1013 (1998)

H. Shen, H. Toki, K. Oyamatsu, K. Sumiyoshi, Astrophys. J. Suppl. 197, 20 (2011)

Thomas-Fermi with RMF (TM1)

H. Togashi, K. Nakazato, Y. Takehara, S. Yamamuro, H. Suzuki, M. Takano, NPA 961 (2017) 78

Thomas-Fermi with realistic nuclear forces

nuclear statistical equilibrium (NSE)

M. Hempel and J. Schaffner-Bielich, Nucl. Phys. A 837, 210 (2010)

A.S. Botvina, I.N. Mishustin, Nucl. Phys. A 843, 98 (2010)

S. Furusawa, K. Sumiyoshi, S. Yamada, H. Suzuki, Astrophys. J. 772, 95 (2013)

S. Typel, G. Ropke, T. Klahn, D. Blaschke, H. Wolter, Phys. Rev. C 81, 015803 (2010)

G. Shen, C. J. Horowitz, E. O'Connor, Phys. Rev. C 83, 065808 (2011)

⋮

Motivation to construct EOS table

1991 - 1998 only one EOS

Lattimer-Swesty EOS NPA 535, 331 (1991) Skyrme force

subroutine → supernova simulation code

? ✗ ✓

1997 - 1998 conditions are ready

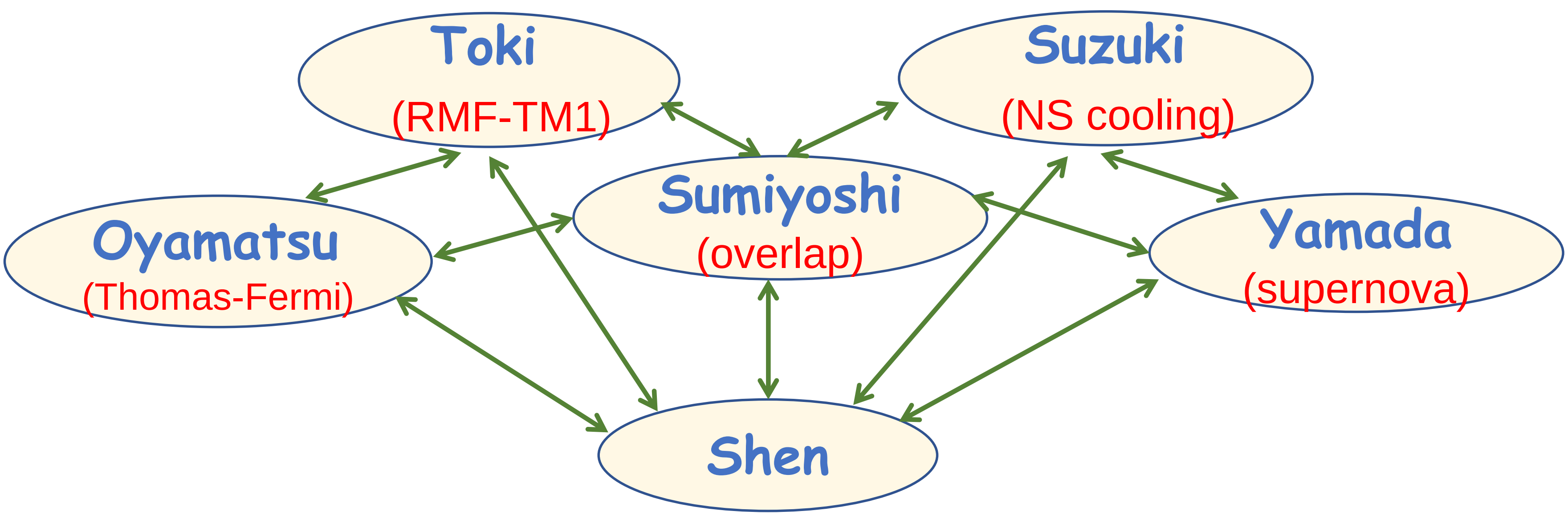

EOS for supernovae

wide range

temperature (T):

0 ~ 100 MeV

proton fraction (Yp):

0 ~ 0.6

density (ρ_B):

10^5 ~ 10^{16} g/cm^3

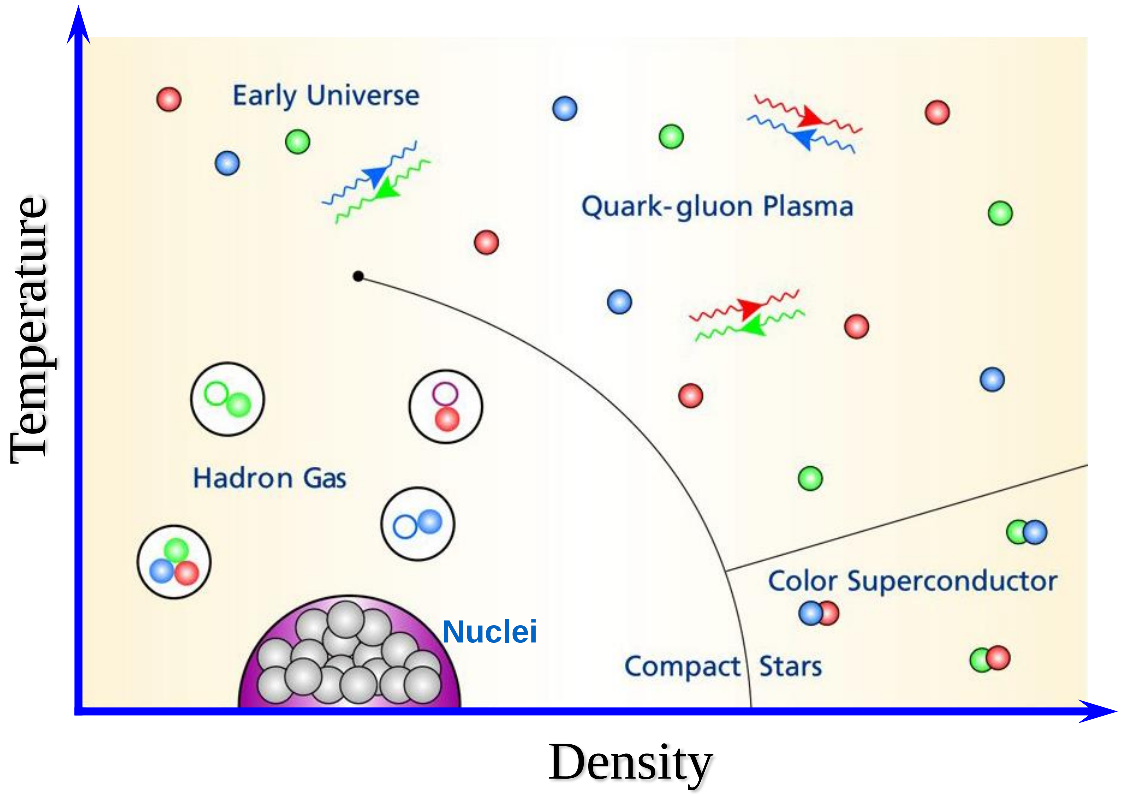

http://www.ice.csic.es/

Models used for EOS

uniform matter

at high density

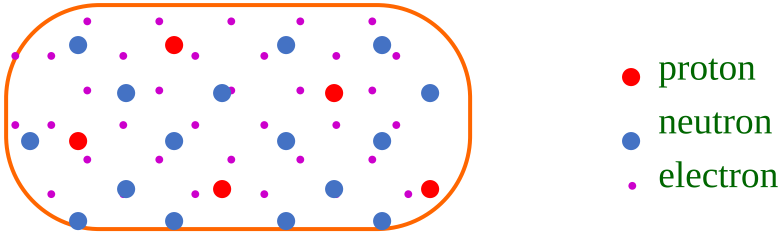

RMF (relativistic Mean Field)

non-uniform matter

at low density

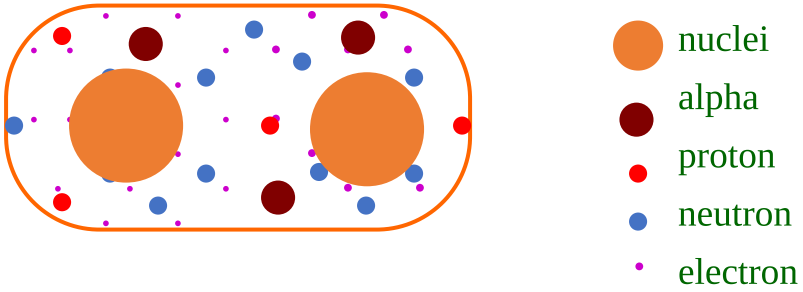

RMF + Thomas-Fermi approximation

Why prefer the RMF theory ?

nuclear many-body methods

nonrelativistic	relativistic
Shell Model	Relativistic Mean-Field (**RMF**)
Skyrme-Hartree-Fock (**SHF**)	Relativistic Hartree-Fock (**RHF**)
Brueckner-Hartree-Fock (**BHF**)	Relativistic Brueckner-Hartree-Fock (**RBHF**)
…	…

Relativity is important!

- natural explanation of spin-orbit force
- natural explanation of three-body force
- good saturation of nuclear matter

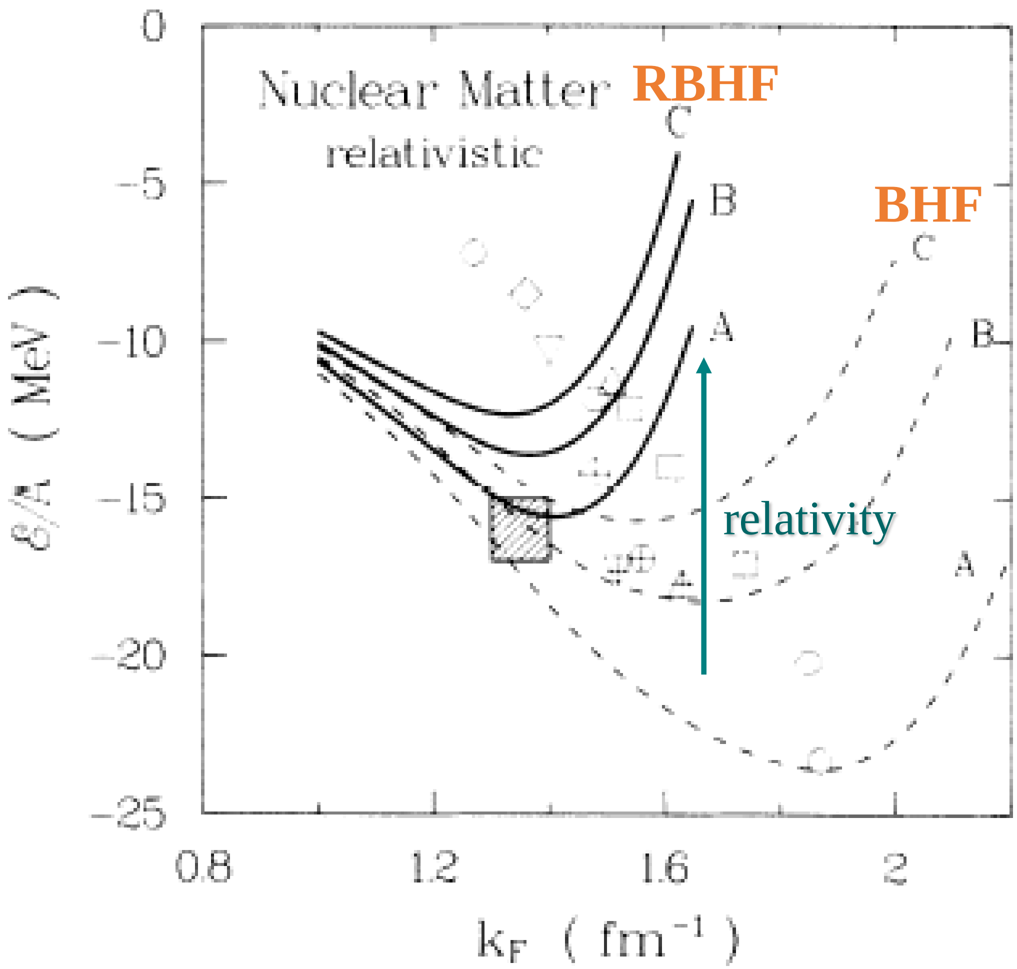

Brockmann, Machleidt, Phys. Rev. C 42 (1990) 1965

Comparison with nuclear data

2157 nuclei

$$\sigma = \sqrt{\frac{\sum_{i=1}^{n}\left(M_{\text{theo}}^{i} - M_{\text{expt}}^{i}\right)^2}{n}}$$
$$= 2.1$$

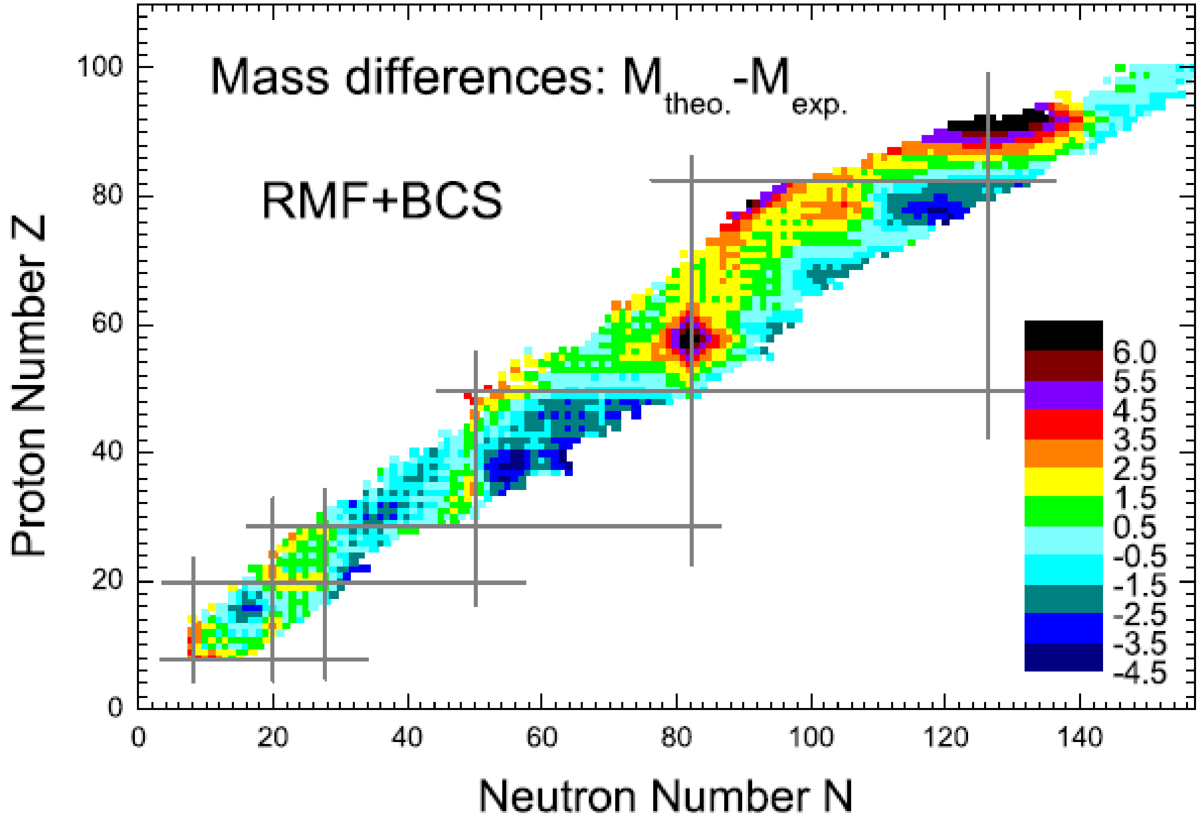

Fig. 2. Mass differences between the predictions of the present work and the experimental data for 2157 nuclei whose measured uncertainties for the masses are less than 0.2 MeV.[34)]

L. S. Geng, H. Toki, J. Meng, Prog. Theor. Phys. 113 (2005) 785

Relativistic Mean Field Theory

Lagrangian

$$L = \overline{\psi}[i\gamma_\mu \partial^\mu - M - g_\sigma \sigma - g_\omega \gamma_\mu \omega^\mu - g_\rho \gamma_\mu \tau_a \rho^{a\mu}]\psi$$
$$+\frac{1}{2}\partial_\mu \sigma \partial^\mu \sigma - \frac{1}{2} m_\sigma^2 \sigma^2 - \frac{1}{3} g_2 \sigma^3 - \frac{1}{4} g_3 \sigma^4$$
$$-\frac{1}{4} W_{\mu\upsilon} W^{\mu\upsilon} + \frac{1}{2} m_\omega^2 \omega_\mu \omega^\mu + \frac{1}{4} c_3 (\omega_\mu \omega^\mu)^2$$
$$-\frac{1}{4} R_{\mu\upsilon}^a R^{a\mu\upsilon} + \frac{1}{2} m_\rho^2 \rho_\mu^a \rho^{a\mu} + \ldots$$

TM1 parameter set

Lagrangian ⇨ Equations ⇨ Mean-Field Approximation

⇩

Calculate everything such as ε , p , s ...

Thomas-Fermi approximation

* body-centered cubic lattice
* parameterized nucleon distribution
* RMF input

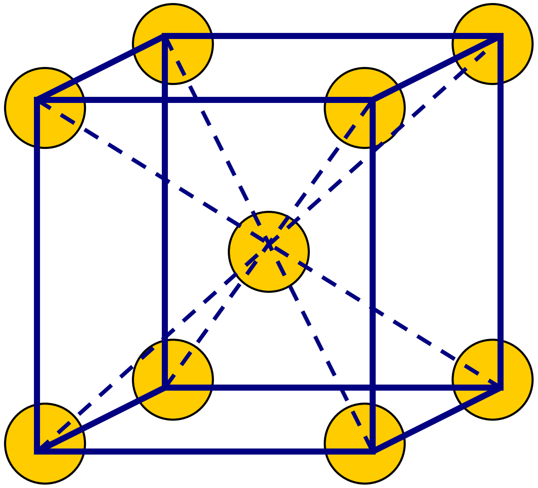

$$E = E_{bulk} + E_{surface} + E_{Coulomb} + E_{Lattice} + E_{electron}$$

assume states → *minimize free energy* → favorable state

EOS tables

EOS1 (1998-version, nucleon)

Shen, Toki, Oyamatsu, Sumiyoshi, Prog. Theor. Phys. 100 (1998) 1013

EOS2 (2010-version, nucleon)

Shen, Toki, Oyamatsu, Sumiyoshi, Astrophys. J. Suppl. 197 (2011) 20

EOS3 (2010-version, nucleon+Λ)

Shen, Toki, Oyamatsu, Sumiyoshi, Astrophys. J. Suppl. 197 (2011) 20

http://phy.nankai.edu.cn/grzy/shenhong/EOS/index.html

http://user.numazu-ct.ac.jp/~sumi/eos/index.html http://phy.nankai.edu.cn/grzy/shenhong/EOS/index.html

Home Page of Relativistic EOS table

Updated information is in readme

Documents

* readme.pdf
* guide_EOS1.pdf
* guide_EOS2.pdf
* guide_EOS3.pdf
* Prog. Theor. Phys. 100 (1998) 1013
* Nucl. Phys. A 637 (1998) 435

EOS table

	EOS1 1998-version nucleon	EOS2 2010-version nucleon	EOS3 2010-version nucleon + Λ
main table	eos1.tab.gz	eos2.tab.zip	eos3.tab.zip
table for T=0	eos1.t00.gz	eos2.t00.zip	eos3.t00.zip
table for Yp=0	eos1.yp0.gz	eos2.yp0.zip	eos3.yp0.zip

Contact

H. Shen
School of Physics, Nankai University,
Tianjin 300071, China
E-mail: shennankai@gmail.com

K. Sumiyoshi
Physics Group, Numazu College of Technology (NCT),
Ooka 3600, Numazu, Shizuoka 410-8501, Japan
E-mail: sumi@numazu-ct.ac.jp

http://user.numazu-ct.ac.jp/~sumi/eos/index.html by K.Sumiyoshi

Home Page of Relativistic EOS table for supernovae

Table of Contents

- **Series of EOS tables based on the RMF framework**
  - Furusawa EOS (2016): Multi-composition of nuclei
    - Nuclear statistical equilibrium (NSE) treatment, extended from Shen EOS table
    - Smooth transition to uniform matter
    - Binding energy shifts for light nuclei
    - Improved shell corrections
  - Shen EOS (2011): Improved version of Shen EOS table:
    - With extended ranges & regular grid points
    - Sets without/with hyperons
  - Furusawa EOS (2011, 2013): Multi-composition of nuclei
    - Nuclear statistical equilibrium (NSE) treatment, extended from Shen EOS table
    - Smooth transition to uniform matter
  - Hyperon EOS (2008): Inclusion of strangeness
    - With hyperons and pions, extended from Shen EOS table
    - Sets with different hyperon-interactions
  - Shen EOS (1998)
    - Original version of Shen EOS table
- **Series of EOS tables based on microscopic approach**
  - Furusawa-Togashi EOS (2017): Multi-compotision of nuclei based on the variational many-body theory
    - Nuclear statistical equilibrium (NSE) treatment, extended from Togashi EOS table
    - Smooth transition to uniform matter
    - Binding energy shifts for light nuclei
    - Improved shell corrections
  - Togashi EOS (2017): Based on the variational many-body theory
    - Starting with realsitic nuclear forces
- **Series of EOS tables with quarks**

Comparison between EOS tables

		1998	2011	2011
		EOS1	EOS2	EOS3
Constituents	Uniform Matter	n, p, α	n, p, α	n, p, α, Λ
	Non-uniform Matter	n, p, α, A	n, p, α, A	n, p, α, A
T	Range	$-1.0 \leq \log_{10}(T) \leq 2.0$	$-1.0 \leq \log_{10}(T) \leq 2.6$	$-1.0 \leq \log_{10}(T) \leq 2.6$
(MeV)	Grid Spacing	$\Delta \log_{10}(T) \simeq 0.1$	$\Delta \log_{10}(T) = 0.04$	$\Delta \log_{10}(T) = 0.04$
	Points	32 (including $T = 0$)	92 (including $T = 0$)	92 (including $T = 0$)
	Range	$-2 \leq \log_{10}(Y_p) \leq -0.25$	$0 \leq Y_p \leq 0.65$	$0 \leq Y_p \leq 0.65$
Y_p	Grid Spacing	$\Delta \log_{10}(Y_p) = 0.025$	$\Delta Y_p = 0.01$	$\Delta Y_p = 0.01$
	Points	72 (including $Y_p = 0$)	66	66
ρ_B	Range	$5.1 \leq \log_{10}(\rho_B) \leq 15.4$	$5.1 \leq \log_{10}(\rho_B) \leq 16$	$5.1 \leq \log_{10}(\rho_B) \leq 16$
(g/cm^3)	Grid Spacing	$\Delta \log_{10}(\rho_B) \simeq 0.1$	$\Delta \log_{10}(\rho_B) = 0.1$	$\Delta \log_{10}(\rho_B) = 0.1$
	Points	104	110	110

- T number of points is increased; upper limit is extended; equal grid is used
- Y_p linear grid is used; upper limit is extended
- ρ_B upper limit is extended; equal grid is used

Phase diagrams

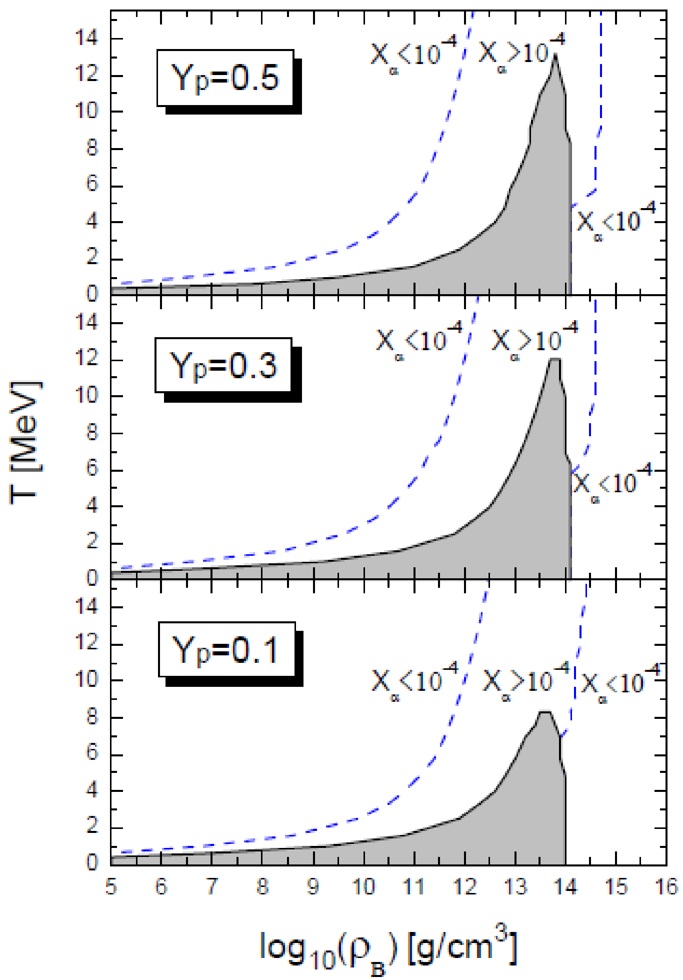

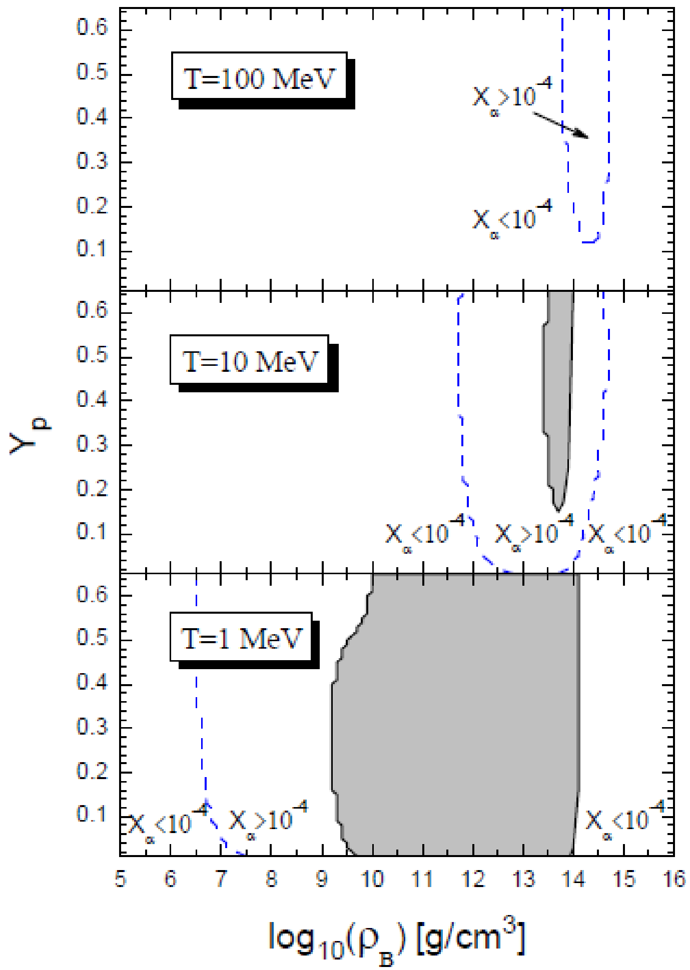

H.Shen, H.Toki, K.Oyamatsu, K.Sumiyoshi, Astrophys. J. Suppl. 197 (2011) 20

Distributions in non-uniform matter

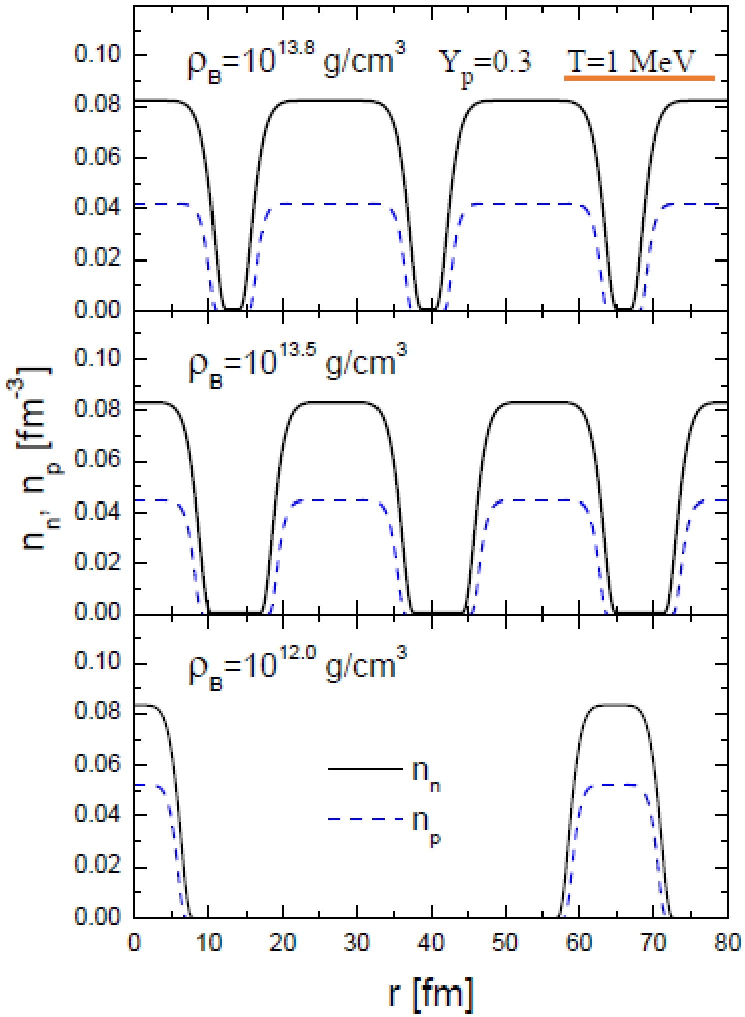

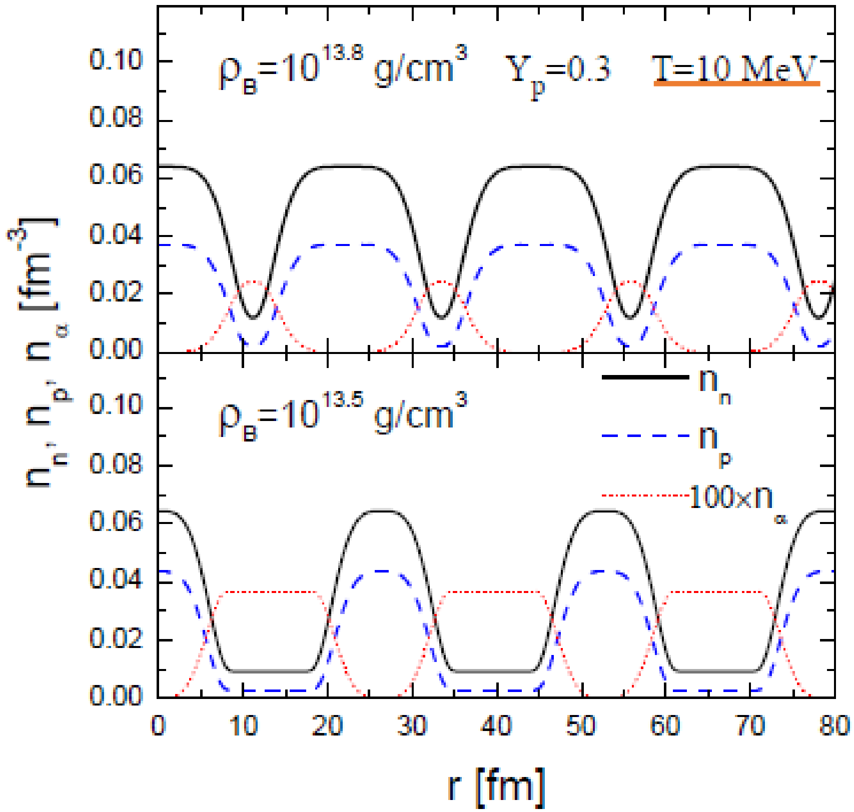

Heavy nuclei in non-uniform matter

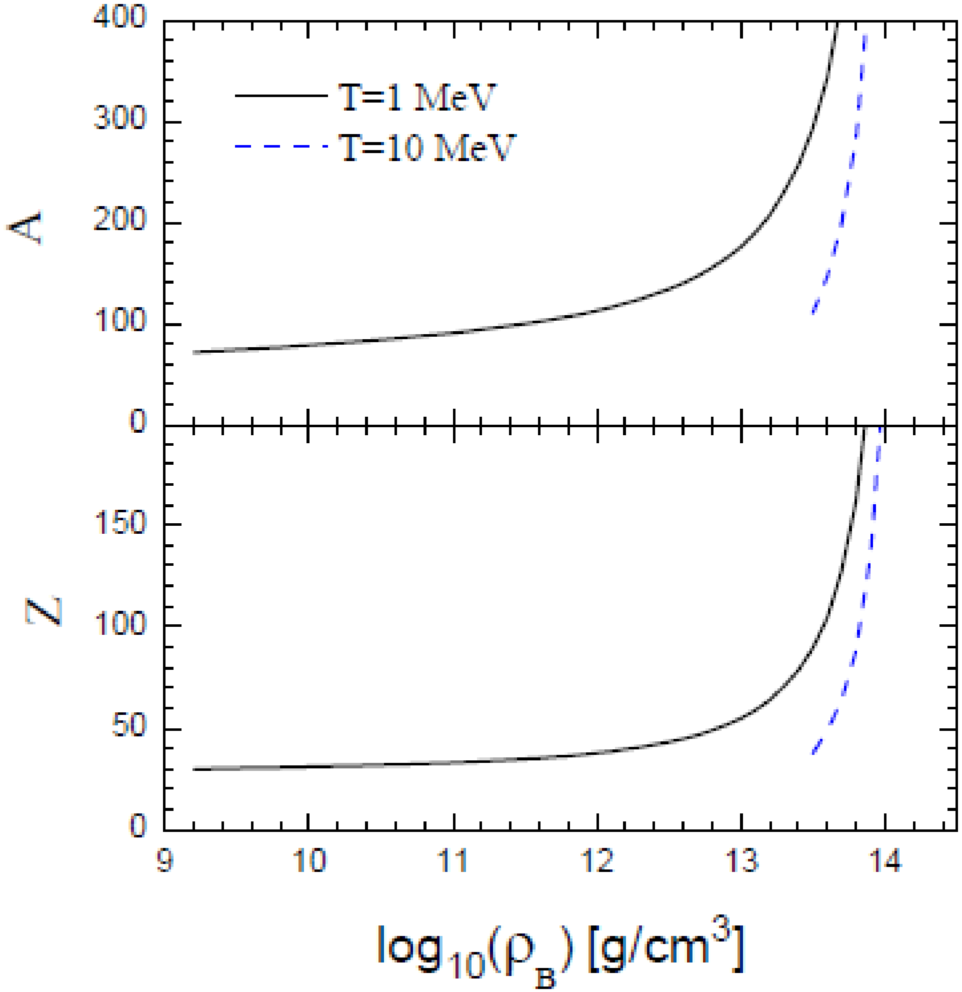

Fractions of components

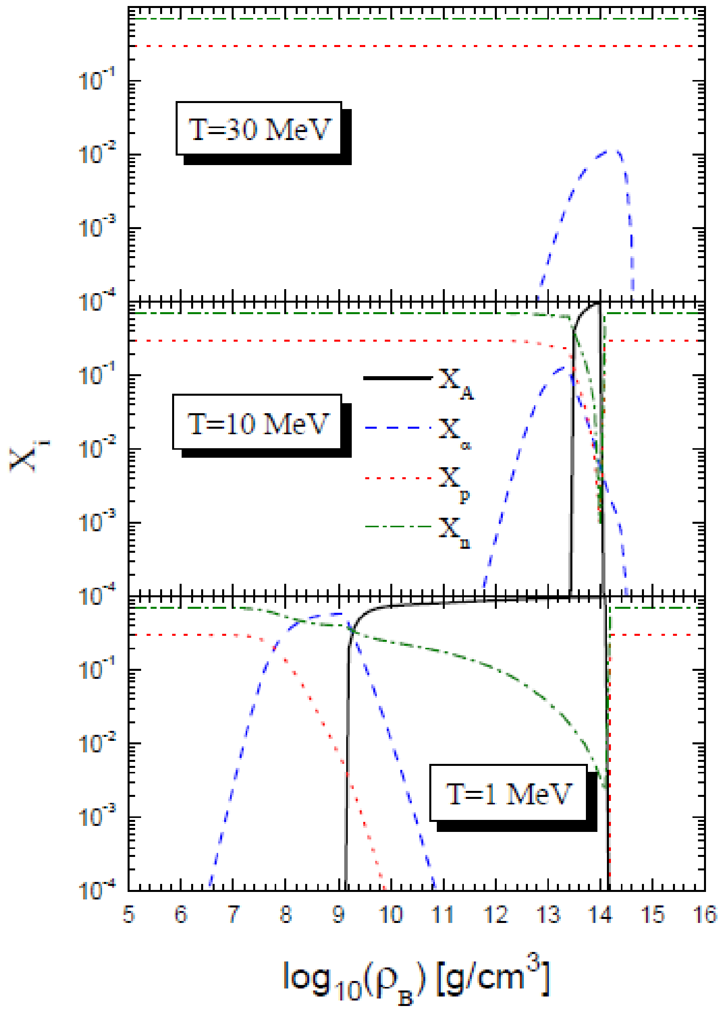

with Λ hyperons

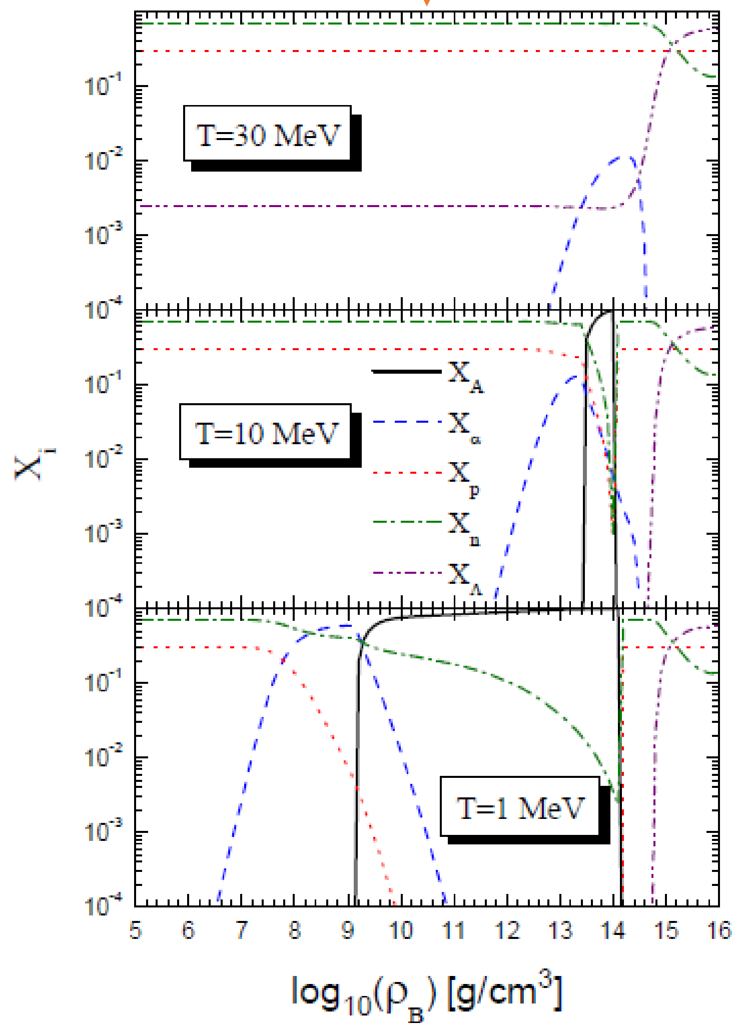

Effects of Λ hyperons

non-nucleonic degrees of freedom

- hyperons: Λ, Σ, Ξ
- boson condensates: π, K
- quarks: u, d, s

EOS for supernovae with hyperons

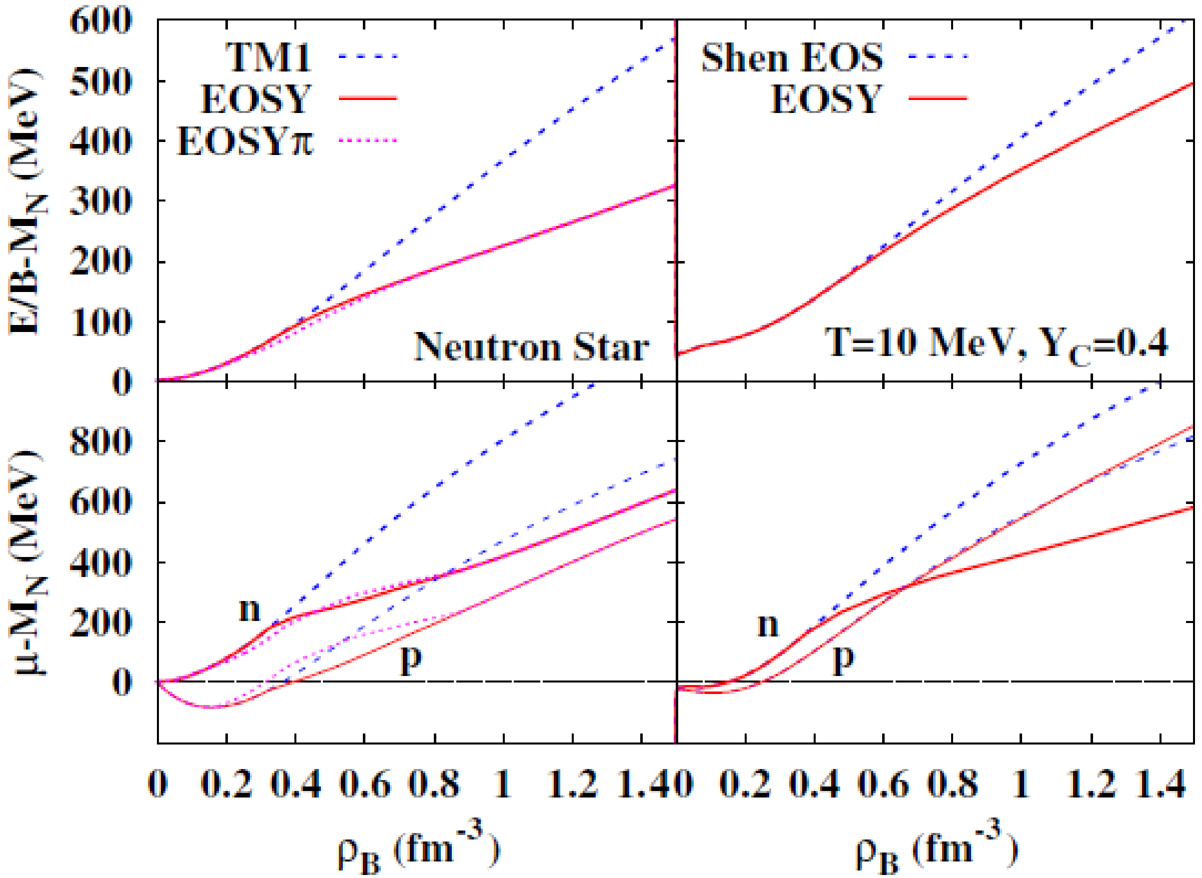

C. Ishizuka, A. Ohnishi, K. Tsubakihara, K. Sumiyoshi, S. Yamada, J. Phys. G 35 (2008) 085201

Pion condensate

PHYSICAL REVIEW C **80**, 038202 (2009)

Possibility of an *s*-wave pion condensate in neutron stars reexamined

A. Ohnishi,[1] D. Jido,[1] T. Sekihara,[2] and K. Tsubakihara[3]
[1] *Yukawa Institute for Theoretical Physics, Kyoto University, Kyoto 606-8502, Japan*
[2] *Department of Physics, Graduate School of Science, Kyoto University, Kyoto 606-8502, Japan*
[3] *Department of Physics, Faculty of Science, Hokkaido University, Sapporo 060-0810, Japan*
(Received 20 October 2008; revised manuscript received 5 September 2009; published 30 September 2009)

We examine possibilities of pion condensation with zero momentum (*s*-wave condensation) in neutron stars by using the pion-nucleus optical potential U and the relativistic mean field (RMF) models. We use low-density phenomenological optical potentials parametrized to fit deeply bound pionic atoms or pion-nucleus elastic scatterings. The proton fraction (Y_p) and electron chemical potential (μ_e) in neutron star matter are evaluated in RMF models. We find that the *s*-wave pion condensation hardly takes place in neutron stars and especially has no chance if hyperons appear in neutron star matter and/or the b_1 parameter in U has density dependence.

Experimental information

scattering experiments

NN scattering data > 4000

YN scattering data ~ 40

no YY scattering data

hypernuclear data

single-Λ hypernuclei > 30

double-Λ hypernuclei ~ 4

single-Σ hypernuclei ~ 1

Hypernuclear Chart

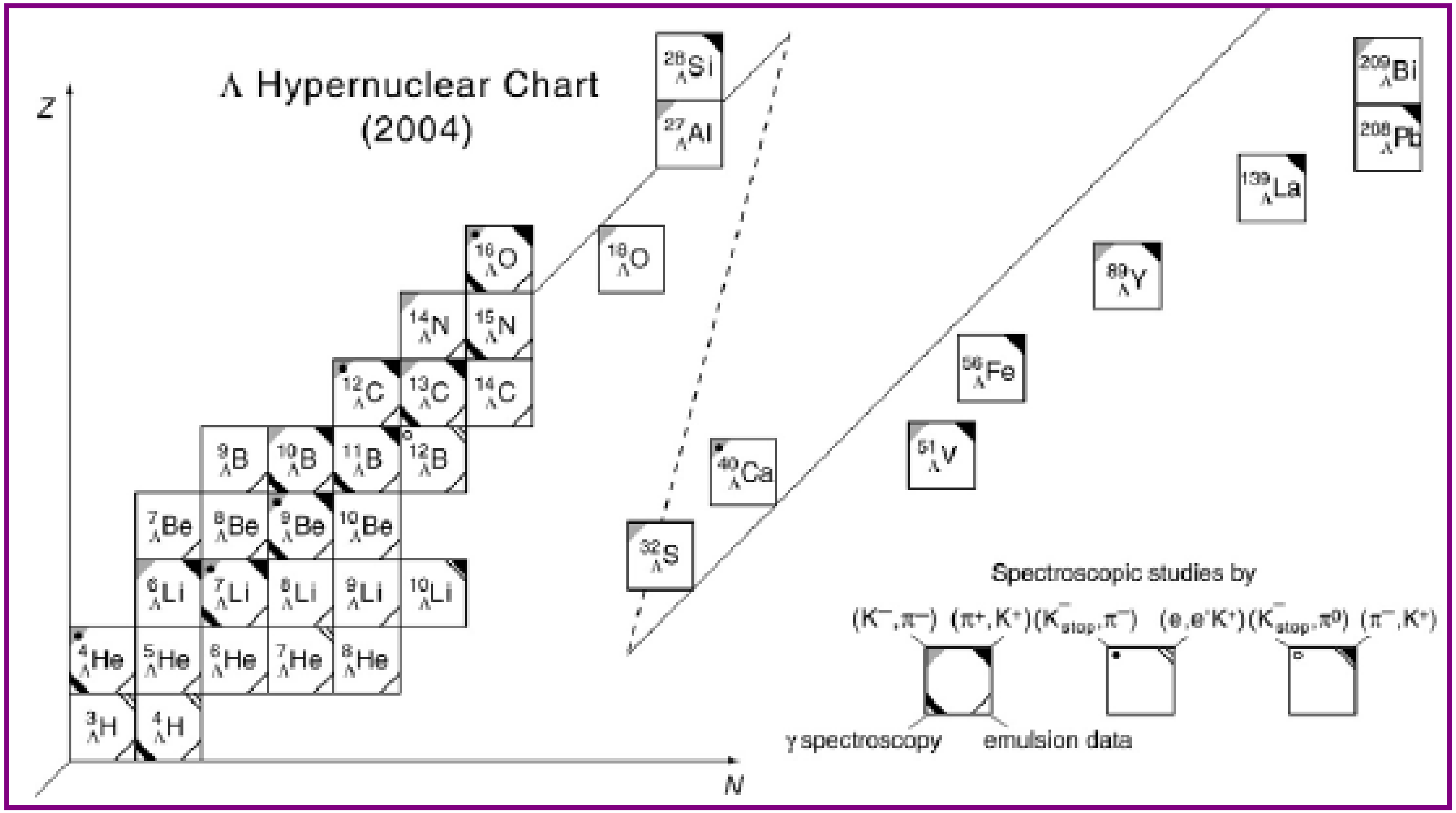

O. Hashimoto, H. Tamura, Prog. Part. Nucl. Phys. 57 (2006) 564

Hypernuclei in the RMF model

Single-Λ hypernuclei

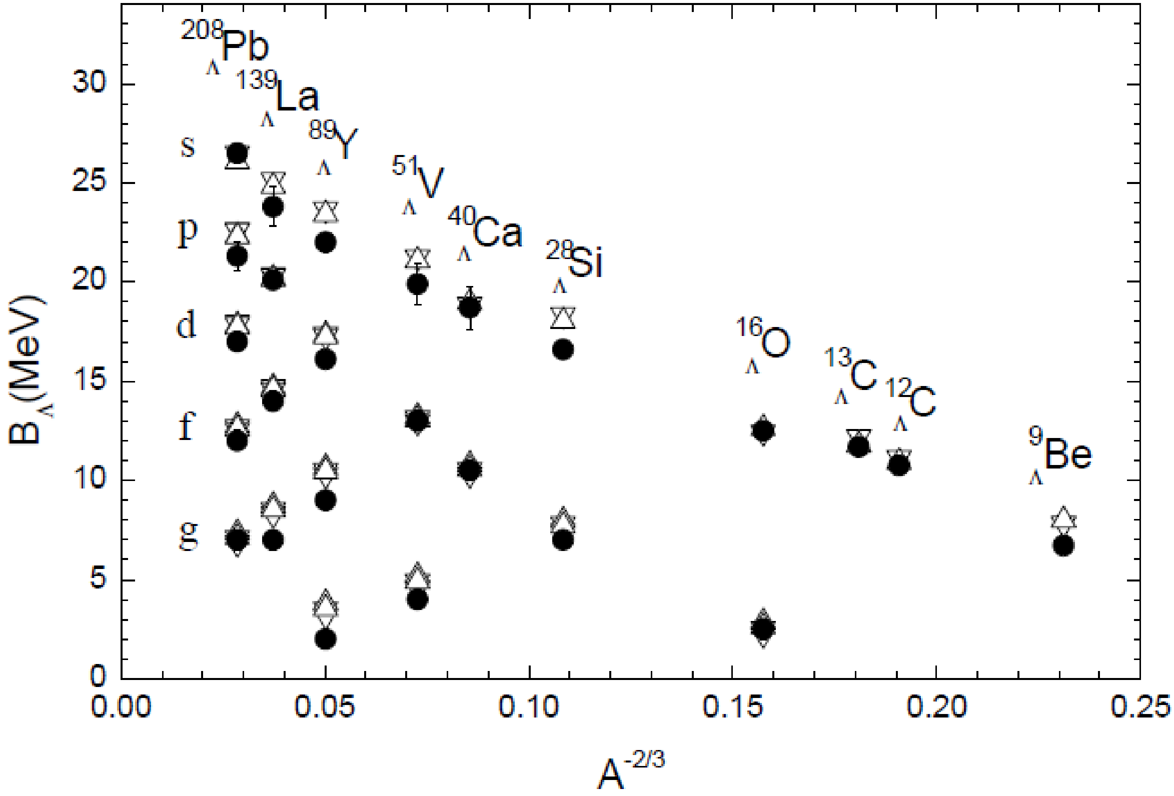

H. Shen, F. Yang, H. Toki, Prog. Theor. Phys. 115 (2006) 325

Hypernuclei in the RMF model

Double-Λ hypernuclei

Table II. $B_{\Lambda\Lambda}$ and $\triangle B_{\Lambda\Lambda}$ of double-Λ hypernuclei. The calculated results of models 1 and 2 are denoted by 1 and 2, respectively. The available experimental data are taken from Refs. 10)–14).

	$B_{\Lambda\Lambda}$	TM1		NL-SH		$\triangle B_{\Lambda\Lambda}$	TM1		NL-SH	
	exp.	1	2	1	2	exp.	1	2	1	2
${}^{6}_{\Lambda\Lambda}$He	7.25 ± 0.2	5.52	5.48	4.75	4.68	1.0 ± 0.2	1.07	1.03	1.08	1.01
${}^{10}_{\Lambda\Lambda}$Be	17.7 ± 0.4	16.34	16.28	16.03	15.94	4.3 ± 0.4	0.37	0.31	0.38	0.29
	14.6 ± 0.4					1.2 ± 0.4				
	8.5 ± 0.7					-4.9 ± 0.7				
${}^{13}_{\Lambda\Lambda}$B	27.5 ± 0.7	22.14	22.07	22.65	22.52	4.8 ± 0.7	0.26	0.19	0.33	0.21
${}^{18}_{\Lambda\Lambda}$O		25.89	25.85	25.30	25.23		0.14	0.10	0.14	0.07
${}^{42}_{\Lambda\Lambda}$Ca		38.15	38.13	37.90	37.86		0.04	0.02	0.04	0.00
${}^{92}_{\Lambda\Lambda}$Zr		47.11	47.10	47.73	47.71		0.03	0.02	0.04	0.02
${}^{210}_{\Lambda\Lambda}$Pb		52.19	52.19	53.03	53.02		0.03	0.02	0.02	0.02

H. Shen, F. Yang, H. Toki, Prog. Theor. Phys. 115 (2006) 325

Effects of Λ hyperons

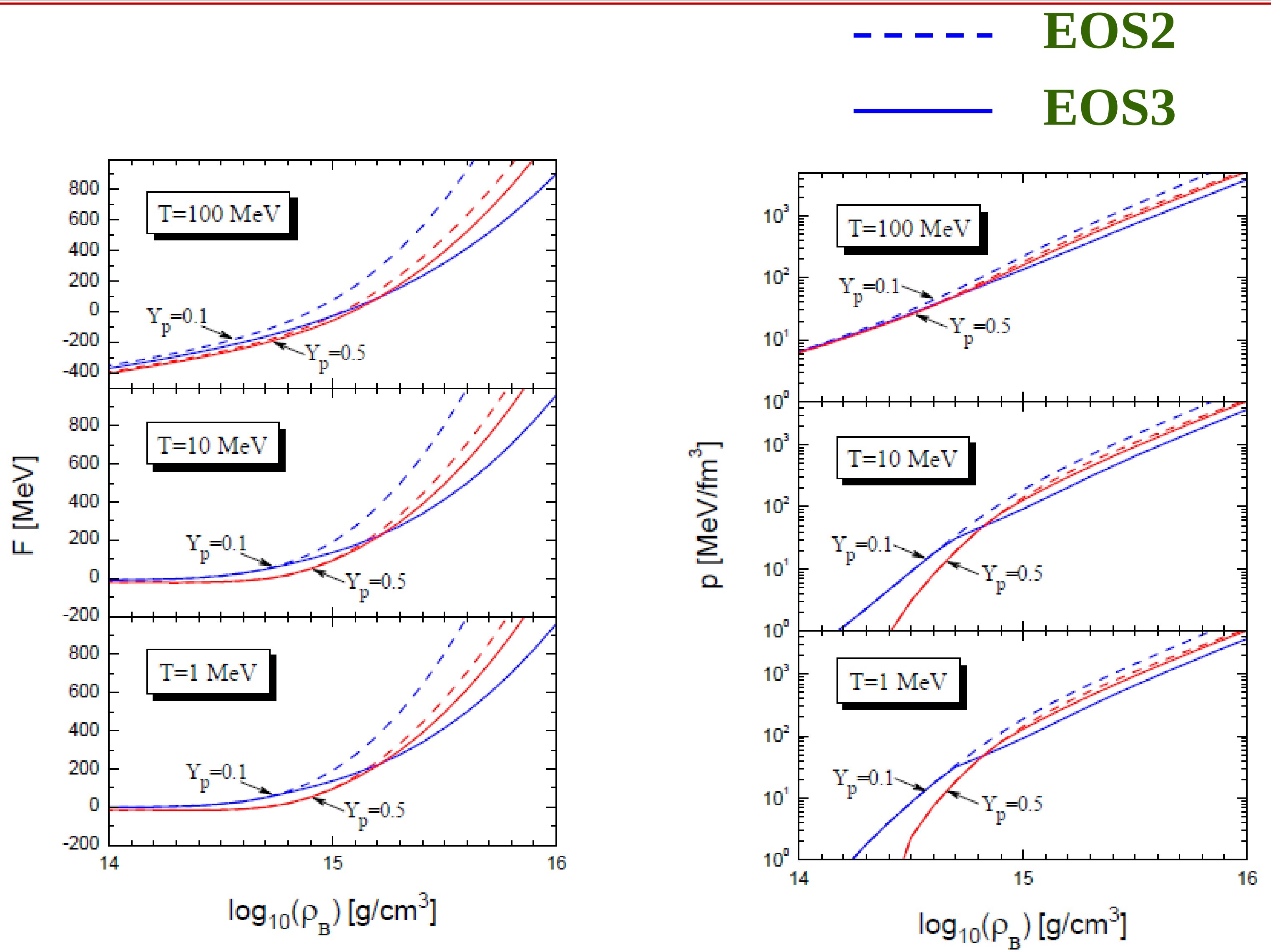

Check of Thomas-Fermi approximation 2014

* parameterized nucleon distribution

$$n_i(r) = \begin{cases} \left(n_i^{in} - n_i^{out}\right)\left[1 - \left(\frac{r}{R_i}\right)^{t_i}\right]^3 + n_i^{out}, & 0 \le r \le R_i \\ n_i^{out}, & R_i \le r \le R_{cell} \end{cases}$$

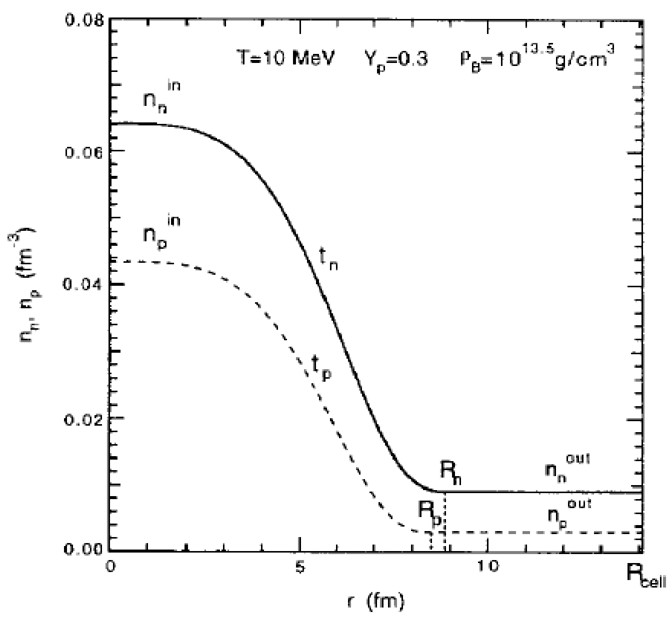

* surface energy

$$E_s = \int_{\text{cell}} F_0 \,|\, \nabla (n_n(r) + n_p(r)) \,|^2 \, d^3 r$$

$$F_0 = 70 \text{ MeV} \cdot \text{fm}^5$$

Check of Thomas-Fermi approximation

Self-consistent Thomas-Fermi approximation

Lagrangian

$$L_{RMF} = \bar{\psi}\left[i\gamma_\mu \partial^\mu - (M + g_\sigma \sigma) - \left(g_\omega \omega + g_\rho \tau_3 \rho + e\frac{\tau_3 + 1}{2} A \right)\gamma^0 \right]\psi$$
$$-\frac{1}{2}(\nabla\sigma)^2 - \frac{1}{2}m_\sigma^2\sigma^2 - \frac{1}{3}g_2\sigma^3 - \frac{1}{4}g_3\sigma^4$$
$$+\frac{1}{2}(\nabla\omega)^2 + \frac{1}{2}m_\omega^2\omega^2 + \frac{1}{4}c_3\omega^4$$
$$+\frac{1}{2}(\nabla\rho)^2 + \frac{1}{2}m_\rho^2\rho^2 + \frac{1}{2}(\nabla A)^2$$
$$+\sum_l \bar{\psi}_l \left(i\gamma_\mu \partial^\mu - m_l + eA\gamma^0 \right)\psi_l$$

Equations

$$-\Delta\sigma + m_\sigma^2\sigma = -g_\sigma\rho_s - g_2\sigma^2 - g_3\sigma^3,$$
$$-\Delta\omega + m_\omega^2\omega = g_\omega\rho_v - c_3\omega^3,$$
$$-\Delta\rho + m_\rho^2\rho = g_\rho\left(\rho_v^p - \rho_v^n\right),$$
$$-\Delta A = e\left(\rho_v^p - \rho_v^l\right).$$

$$M^* = M + g_\sigma\sigma$$
$$\mu_p = \nu_p + g_\omega\omega + g_\rho\rho + eA$$
$$\mu_n = \nu_n + g_\omega\omega - g_\rho\rho$$

Self-consistent Thomas-Fermi approximation

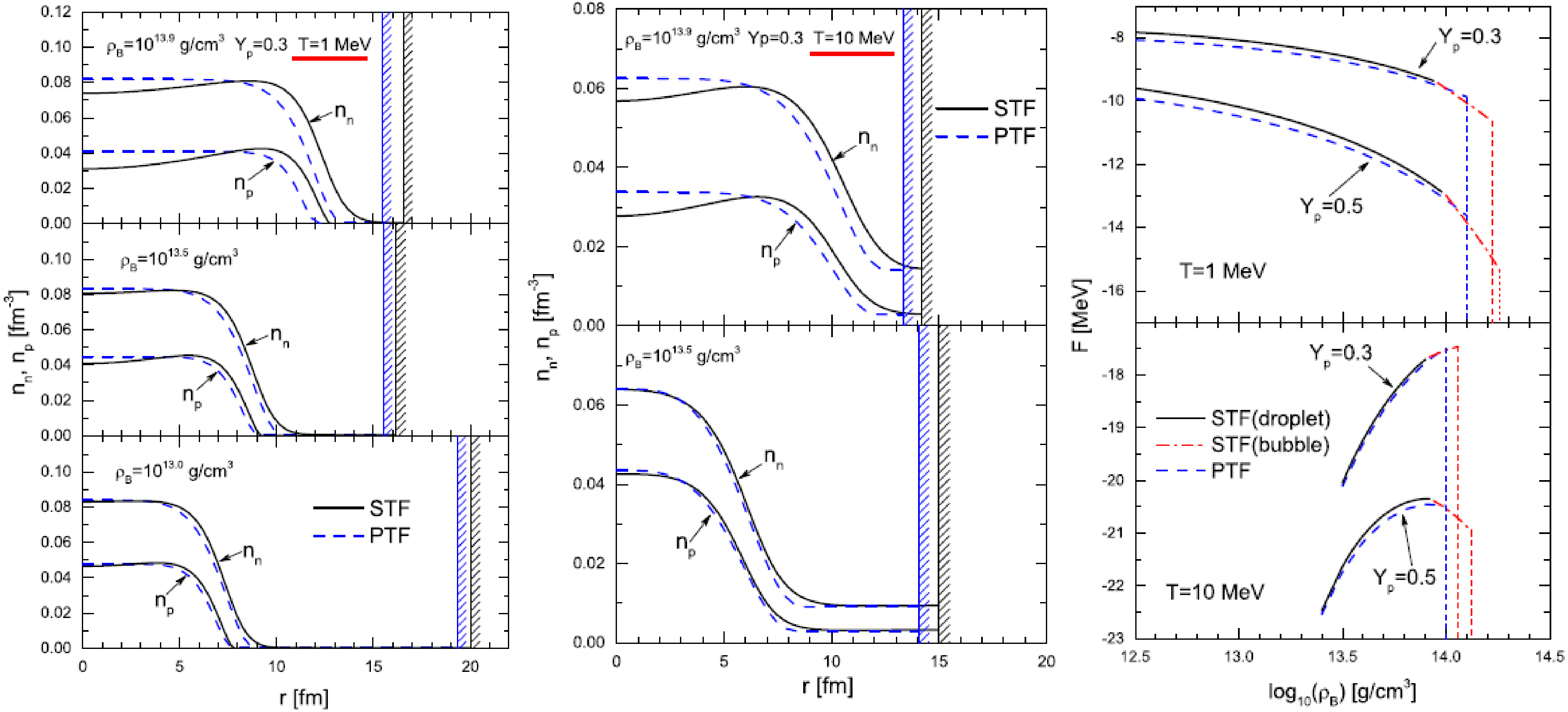

Z. W. Zhang, H. Shen, Astrophys. J. 788 (2014) 185

Self-consistent Thomas-Fermi approximation

Table 2

Comparison between Different Methods for the Cases of $Y_p = 0.3$ and $T = 1$ MeV at $\rho_B = 10^{13.0}$, $10^{13.5}$, and $10^{13.9}$ g cm^{-3}

$\log_{10}(\rho_B)$ (g cm^{-3})	Method	F (MeV)	E (MeV)	S (k_B)	E_b (MeV)	E_g (MeV)	E_C (MeV)	R_c (fm)
13.0	STF	−8.087	−7.807	0.280	−10.135	1.164	1.164	20.0
	PTF ($F_0 = 70$)	−8.304	−8.025	0.278	−10.161	1.068	1.068	19.3
	PTF ($F_0 = 90$)	−8.023	−7.748	0.275	−10.080	1.166	1.166	20.3
13.5	STF	−8.577	−8.377	0.201	−10.275	0.949	0.949	16.1
	PTF ($F_0 = 70$)	−8.754	−8.554	0.200	−10.286	0.866	0.866	15.5
	PTF ($F_0 = 90$)	−8.527	−8.326	0.200	−10.223	0.948	0.948	16.3
13.9	STF	−9.275	−9.112	0.163	−10.433	0.660	0.660	16.6
	PTF ($F_0 = 70$)	−9.388	−9.226	0.162	−10.438	0.606	0.606	15.5
	PTF ($F_0 = 90$)	−9.229	−9.066	0.164	−10.386	0.660	0.660	16.4

PTF ($F_0 = 90$ MeV $\cdot$ fm^5) **≈ SPF**

symmetry energy effects

* energy per particle w as function of n and $\alpha = \frac{n_n - n_p}{n}$

$$w = w_0 + \frac{K_0}{18n_0^2}(n-n_0)^2 + \left[S_0 + \frac{L}{3n_0}(n-n_0)\right]\alpha^2$$

symmetry energy slope $L = \left[3n\frac{\partial E_{\rm sym}(n)}{\partial n}\right]_{n=n_0}$

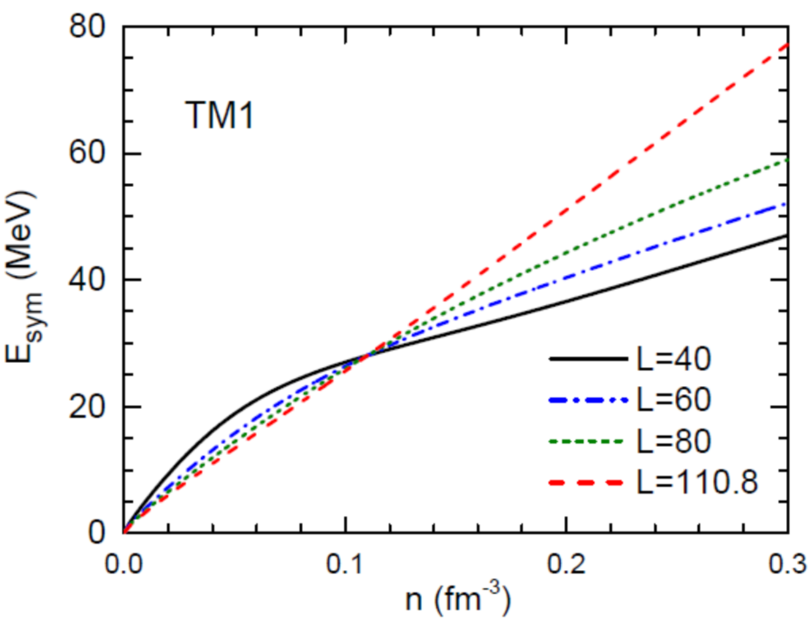

symmetry energy effects

* generated RMF models with different L by turning g_ρ and Λ_v

$$
\begin{aligned}
\mathcal{L}_{\rm RMF} = & \bar{\psi}\left[i\gamma_\mu\partial^\mu - (M + g_\sigma\sigma) - \left(g_\omega\omega^\mu + \frac{g_\rho}{2}\tau_a\rho^{a\mu}\right)\gamma_\mu\right]\psi \\
& + \frac{1}{2}\partial_\mu\sigma\partial^\mu\sigma - \frac{1}{2}m_\sigma^2\sigma^2 - \frac{1}{3}g_2\sigma^3 - \frac{1}{4}g_3\sigma^4 \\
& - \frac{1}{4}W_{\mu\nu}W^{\mu\nu} + \frac{1}{2}m_\omega^2\omega_\mu\omega^\mu + \frac{1}{4}c_3\left(\omega_\mu\omega^\mu\right)^2 \\
& - \frac{1}{4}R^a_{\mu\nu}R^{a\mu\nu} + \frac{1}{2}m_\rho^2\rho^a_\mu\rho^{a\mu} + \Lambda_{\rm v}\left(g_\omega^2\omega_\mu\omega^\mu\right)\left(g_\rho^2\rho^a_\mu\rho^{a\mu}\right)
\end{aligned}
$$

* all models have the same isoscalar saturation properties

TABLE II. Parameters g_ρ and Λ_v generated from the TM1 model for different slope L at saturation density n_0 with fixed symmetry energy $E_{\rm sym} = 28.05$ MeV at $n_{\rm fix} = 0.11\ {\rm fm}^{-3}$. The last two lines show the symmetry energy at saturation density, $E_{\rm sym}(n_0)$, and the neutron-skin thickness of ^{208}Pb, Δr_{np}. The original TM1 model has $L = 110.8$ MeV.

L (MeV)	40.0	50.0	60.0	70.0	80.0	90.0	100.0	110.8
g_ρ	13.9714	12.2413	11.2610	10.6142	10.1484	9.7933	9.5114	9.2644
Λ_v	0.0429	0.0327	0.0248	0.0182	0.0128	0.0080	0.0039	0.0000
$E_{\rm sym}(n_0)$ (MeV)	31.38	32.39	33.29	34.11	34.86	35.56	36.22	36.89
Δr_{np} (fm)	0.1574	0.1886	0.2103	0.2268	0.2402	0.2514	0.2609	0.2699

S. S. Bao, J. N. Hu, Z. W. Zhang, H. Shen, Phys. Rev. C 90 (2014) 045802

symmetry energy and finite size effects

liquid-gas phase transition in supernova matter

* **spinodal instability** (no surface and Coulomb)
  determined by the curvature of the free energy

* **bulk calculation** (no surface and Coulomb)
  phase equilibrium determined by the Gibbs conditions

* **coexisting phases (CP)** (surface and Coulomb perturbatively)
  phase equilibrium determined by the Gibbs conditions

* **compressible liquid-drop (CLD)** (minimization of free energy)
  phase equilibrium determined by minimization

* **Thomas-Fermi (TF)** (realistic description)

symmetry energy and finite size effects

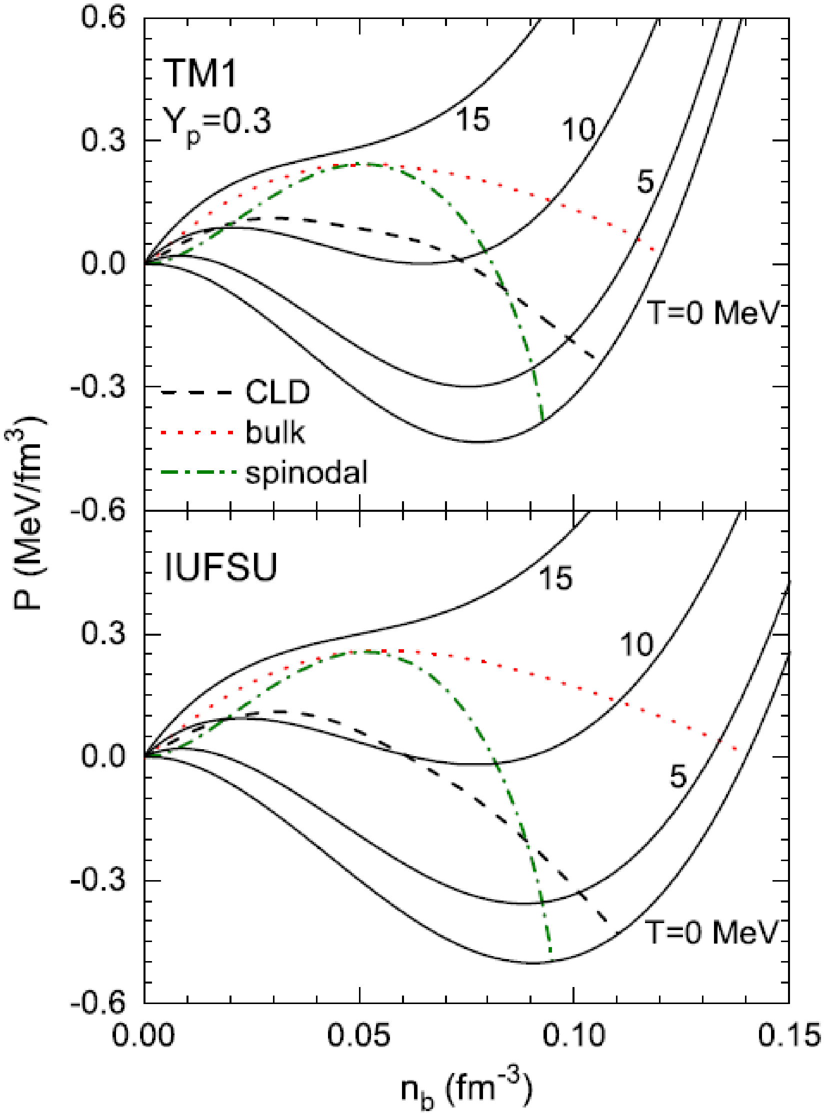

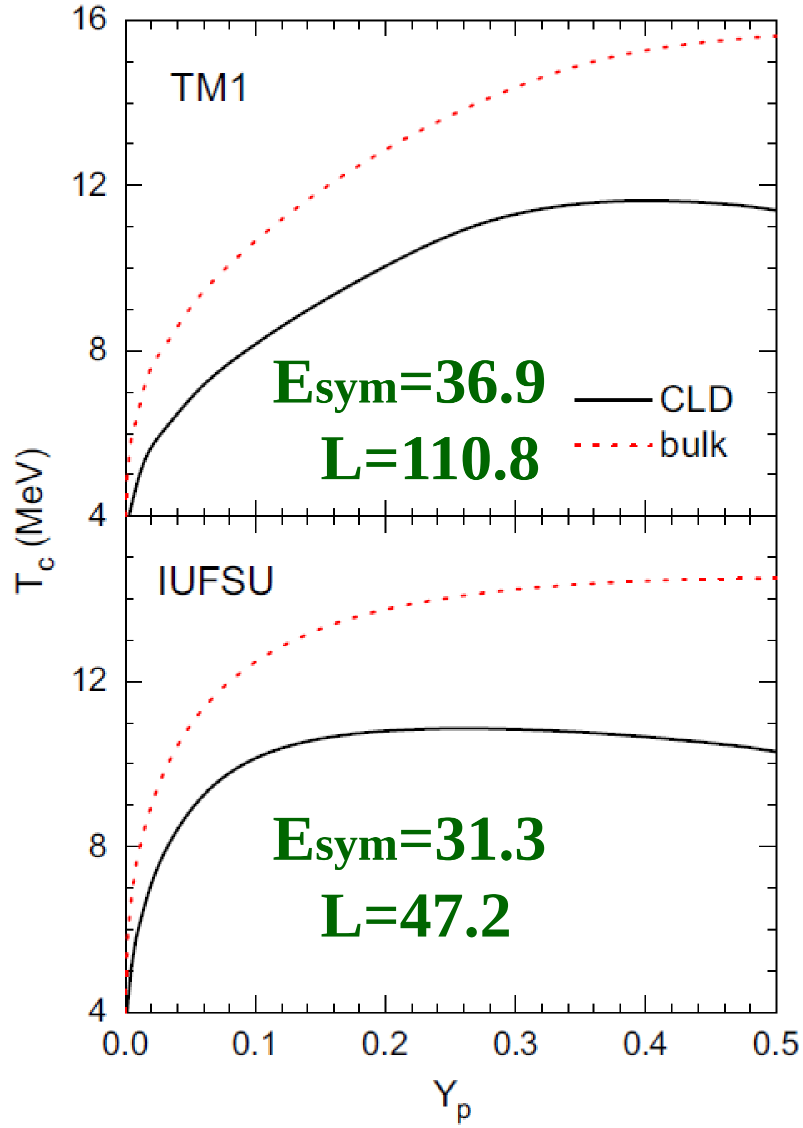

S. S. Bao and H. Shen, Phys. Rev. C9 3 (2016) 025807

symmetry energy and finite size effects

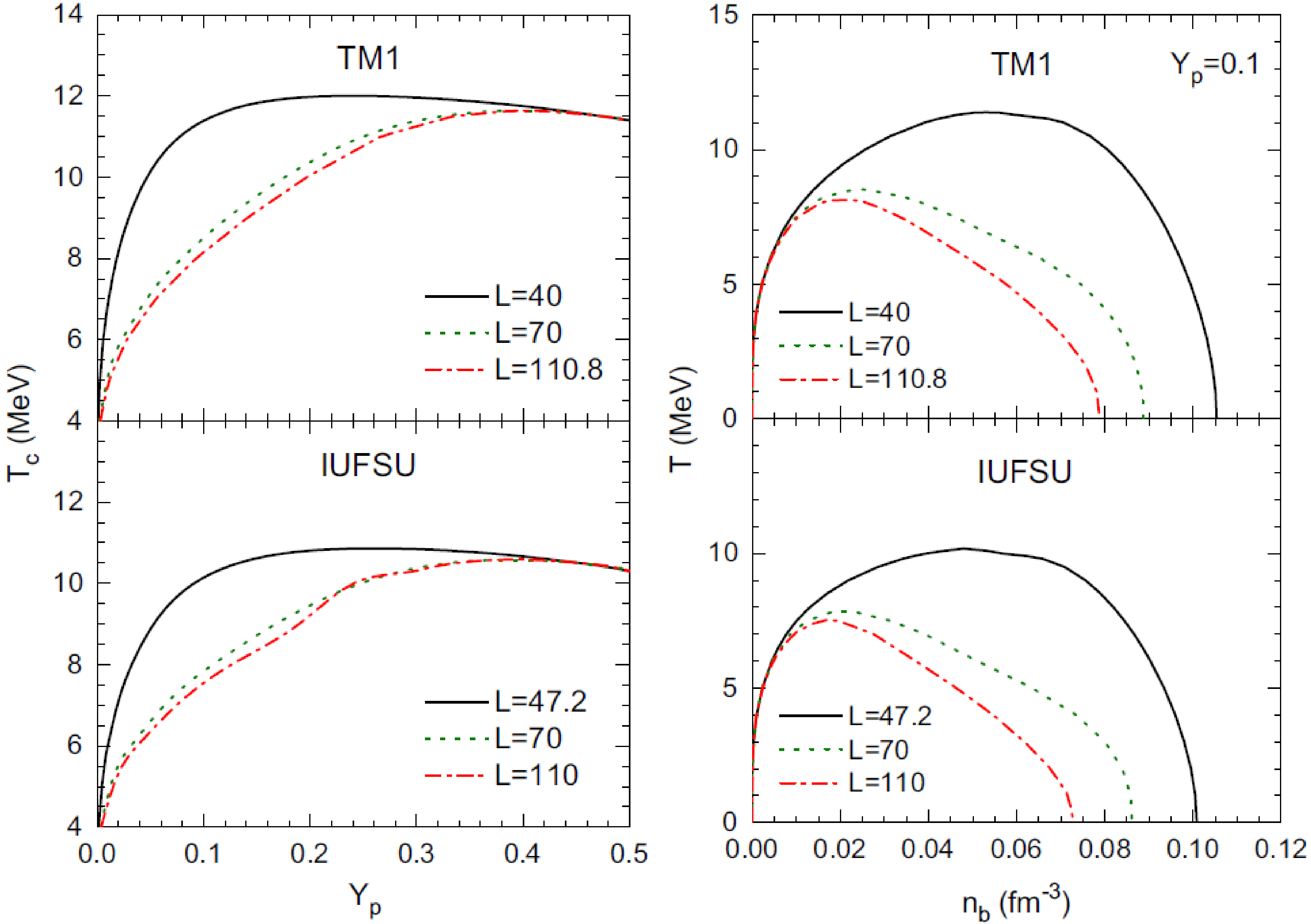

symmetry energy and finite size effects

pressure & L

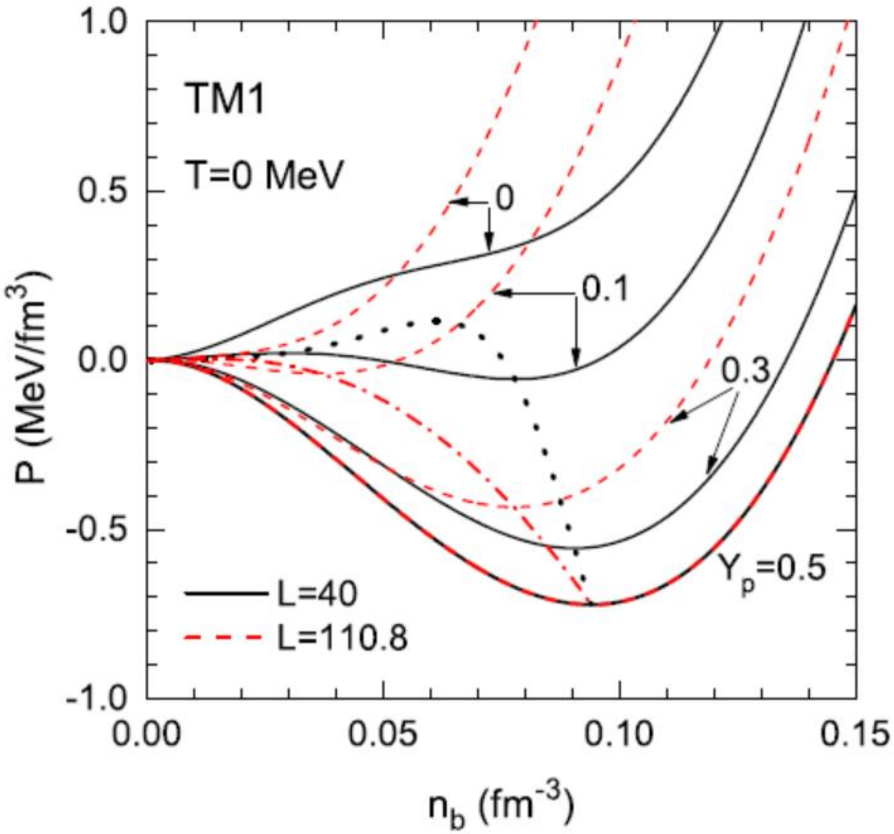

FIG. 8. Pressure of uniform matter P as a function of baryon density n_b at zero temperature for various proton fraction Y_p. The black solid and red dashed lines are the results of $L = 40$ MeV and $L = 110.8$ MeV in the TM1 set, respectively. The dotted and dashed-dotted lines indicate the mechanically unstable regions from negative compressibility ($dP/dn_b < 0$).

surface tension & L

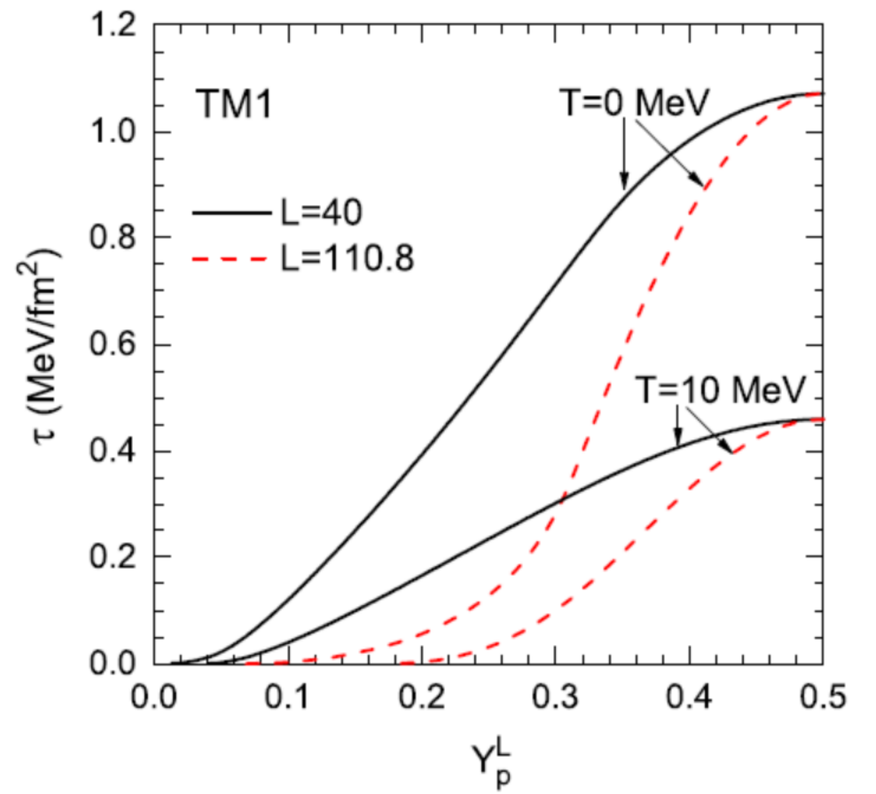

FIG. 10. Surface tension τ as a function of proton fraction in the liquid phase Y_p^L at $T = 0$ and 10 MeV using the models with $L = 40$ and 110.8 MeV in the TM1 set.

symmetry energy and neutron stars

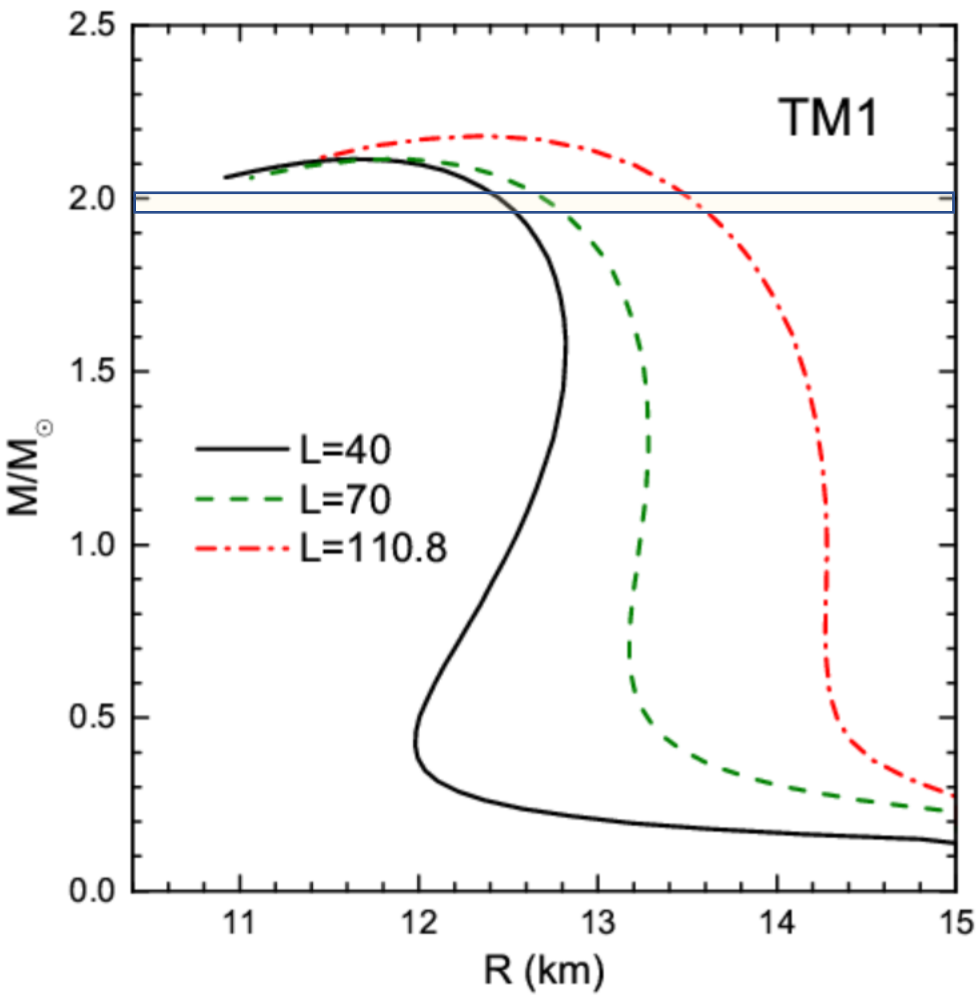

smaller L corresponds to smaller R

symmetry energy and neutron stars

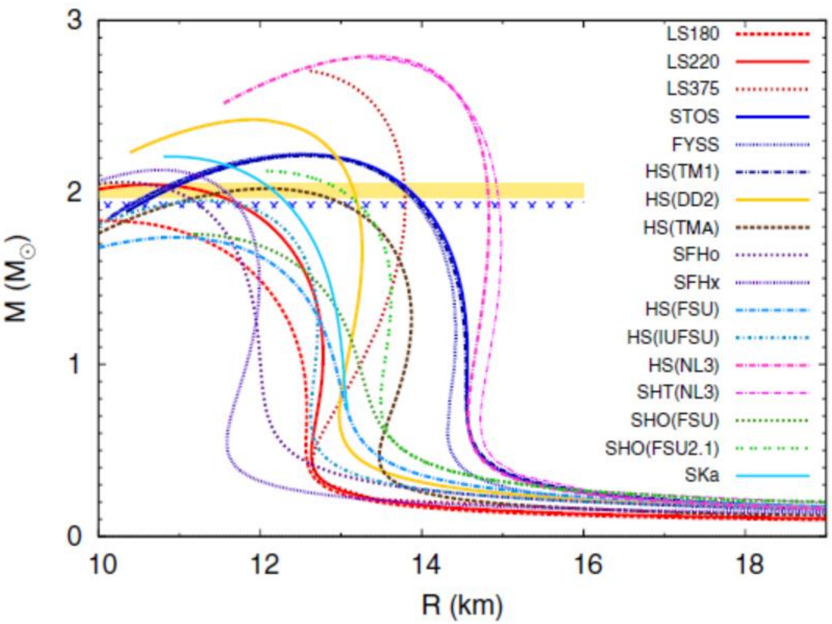

Nuclear interaction	n_{sat} (fm^{-3})	B_{sat} (MeV)	K (MeV)	Q (MeV)	J (MeV)	L (MeV)
SKa	0.155	16.0	263	−300	32.9	74.6
LS180	0.155	16.0	180	−451	28.6[a]	73.8
LS220	0.155	16.0	220	−411	28.6[a]	73.8
LS375	0.155	16.0	375	176	28.6[a]	73.8
TM1	0.145	16.3	281	−285	36.9	110.8
TMA	0.147	16.0	318	−572	30.7	90.1
NL3	0.148	16.2	272	203	37.3	118.2
FSUgold	0.148	16.3	230	−524	32.6	60.5
FSUgold2.1	0.148	16.3	230	−524	32.6	60.5
IUFSU	0.155	16.4	231	−290	31.3	47.2
DD2	0.149	16.0	243	169	31.7	55.0
SFHo	0.158	16.2	245	−468	31.6	47.1
SFHx	0.160	16.2	239	−457	28.7	23.2

M. Oertel, M. Hempel, T. Klähn, S. Typel, Rev. Mod. Phys. 89, 015007 (2017)

smaller L corresponds to smaller R

EOS for neutron stars

$T = 0, \quad \rho \sim 10^{7} - 10^{15}\ \text{g/cm}^3$

non-uniform matter → uniform matter

$e+A \rightarrow e+n+A \longrightarrow (e,\mu)+(n,p) \rightarrow + \begin{cases} \textit{hyperons} \\ \textit{quarks} \\ \dots \end{cases}$

$\rho \sim 10^{11}\ \text{g/cm}^3 \qquad \rho \sim 10^{14}\ \text{g/cm}^3$

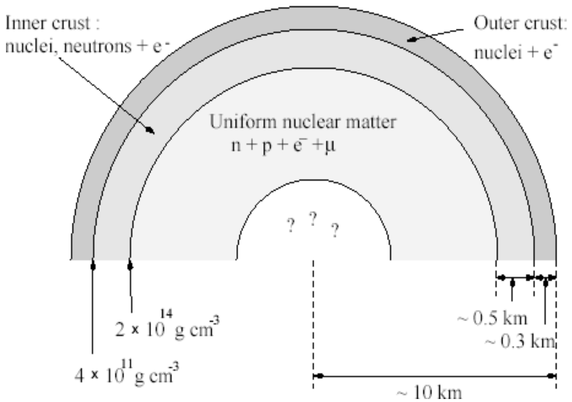

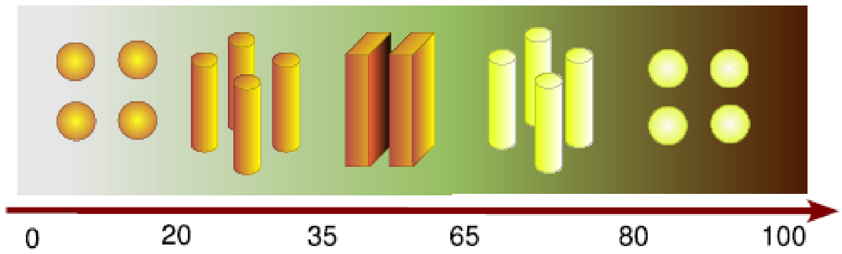

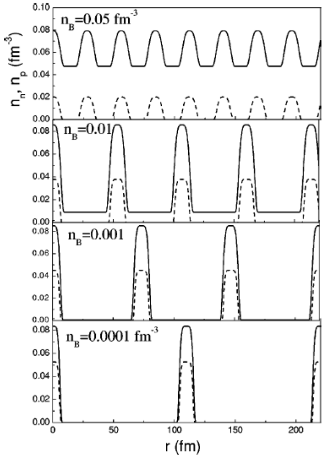

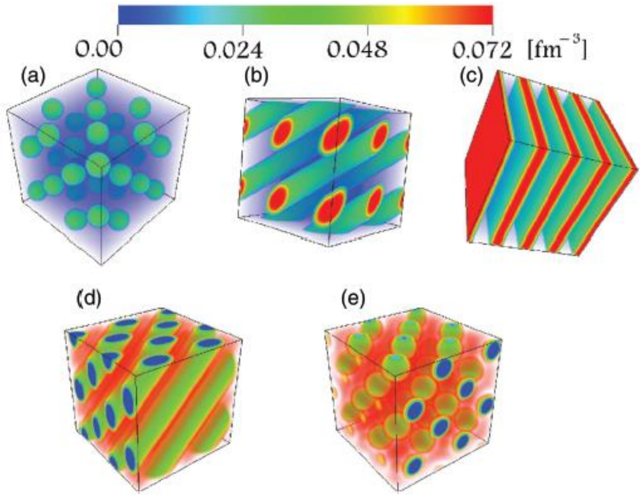

H. Shen, PRC 65 (2002) 035802

M.Okamoto, T.Maruyama, K.Yabana, T.Tatsumi, PRC 88 (2013) 025801

Symmetry energy ↔ pasta phases, crust-core

K. Oyamatsu, K. Iida, Phys. Rev. C 75, 015801 (2007)
B. A. Li, L. W. Chen, C. M. Ko, Phys. Rep. 464, 113 (2008)
F. Grill, C. Providência, S. S. Avancini, Phys. Rev. C 85, 055808 (2012)
Z. Zhang, L. W. Chen, Phys. Lett. B 726, 234 (2013)
S. S. Bao, H. Shen, Phys. Rev. C 89, 045807 (2014)
S. S. Bao, J. N. Hu, Z. W. Zhang, H. Shen, Phys. Rev. C 90, 045802 (2014)
S. S. Bao, H. Shen, Phys. Rev. C 91, 015807 (2015)

adjust g_ρ, Λ_V → fix symmetry energy at 0.11 fm^{-3}, different symmetry energy slope L → saturation property, neutron star mass ~2 $M_\odot$, finite nuclei

TM1 set →

L (MeV)	40.0	50.0	60.0	70.0	80.0	90.0	100.0	110.8
g_ρ	13.9714	12.2413	11.2610	10.6142	10.1484	9.7933	9.5114	9.2644
Λ_V	0.0429	0.0327	0.0248	0.0182	0.0128	0.0080	0.0039	0.0000

IUFSU set →

L (MeV)	47.2	50.0	60.0	70.0	80.0	90.0	100.0	110.0
g_ρ	13.5900	12.8202	11.1893	10.3150	9.7537	9.3559	9.0558	8.8192
Λ_V	0.0460	0.0420	0.0305	0.0220	0.0153	0.0098	0.0051	0.0011

S. S. Bao, H. Shen, Phys. Rev. C 91, 015807 (2015)

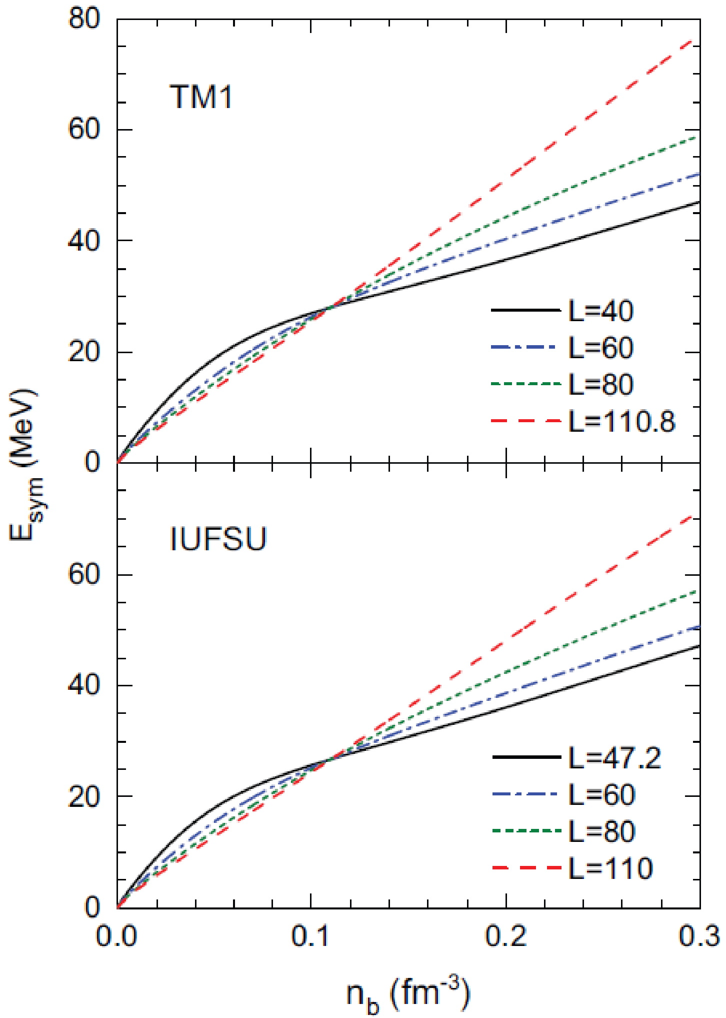

symmetry energy

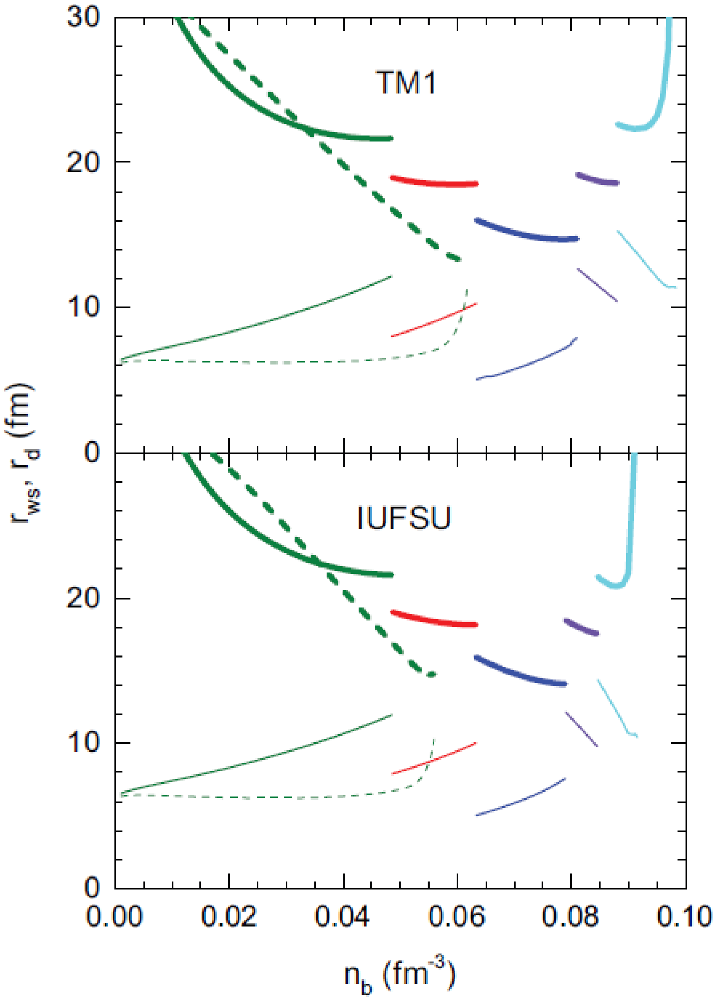

size of Wigner-Seitz cell
size of pasta structure

distributions of neutrons and protons

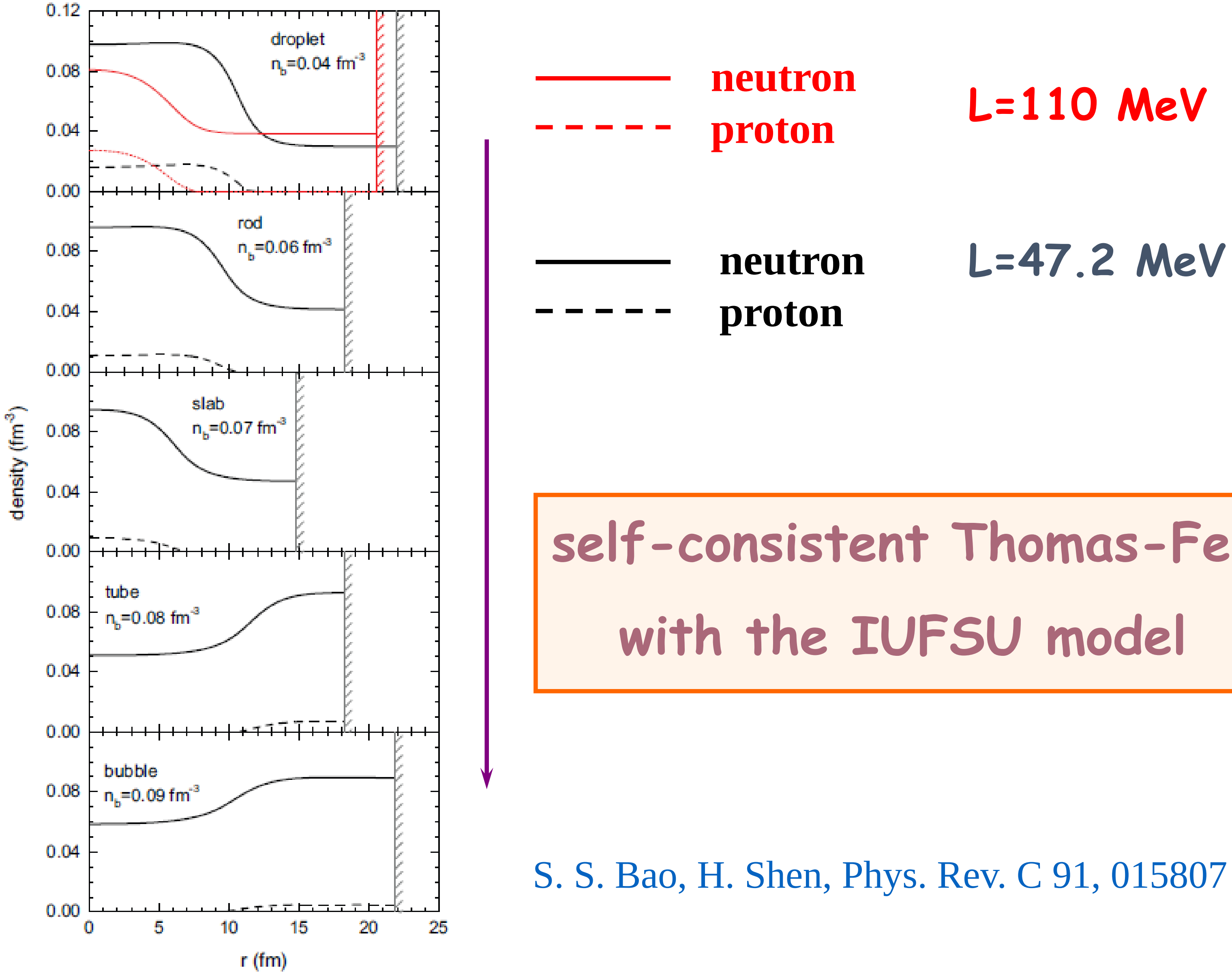

self-consistent Thomas-Fermi with the IUFSU model

S. S. Bao, H. Shen, Phys. Rev. C 91, 015807 (2015)

Crust-core transition

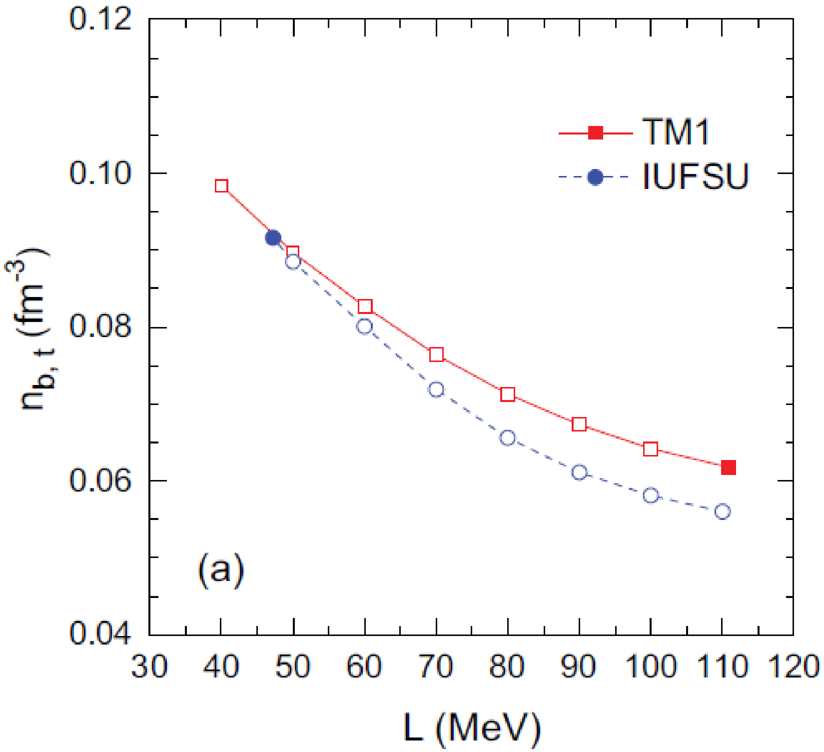

transition density

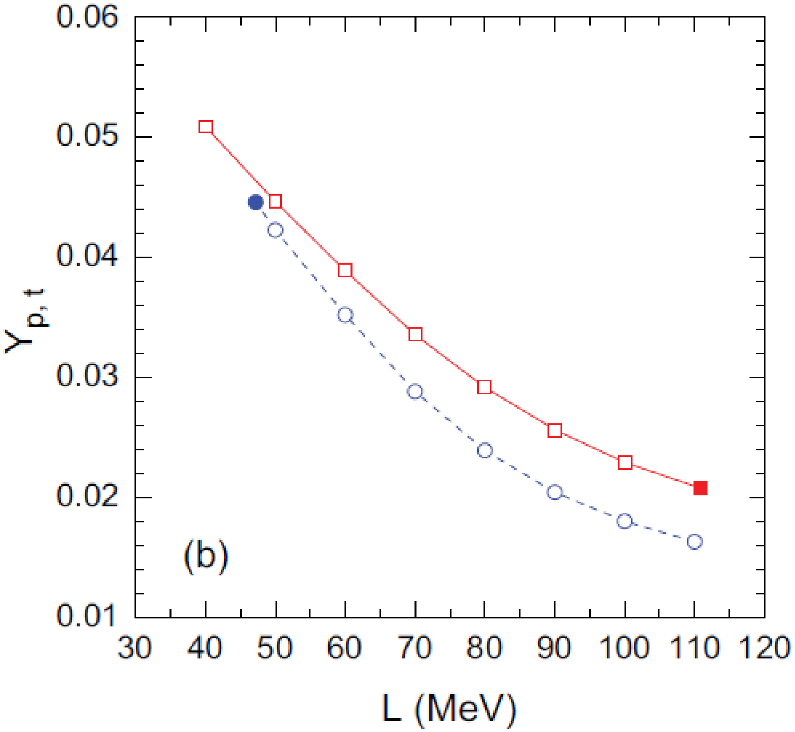

proton fraction

Phase diagram of inner crust

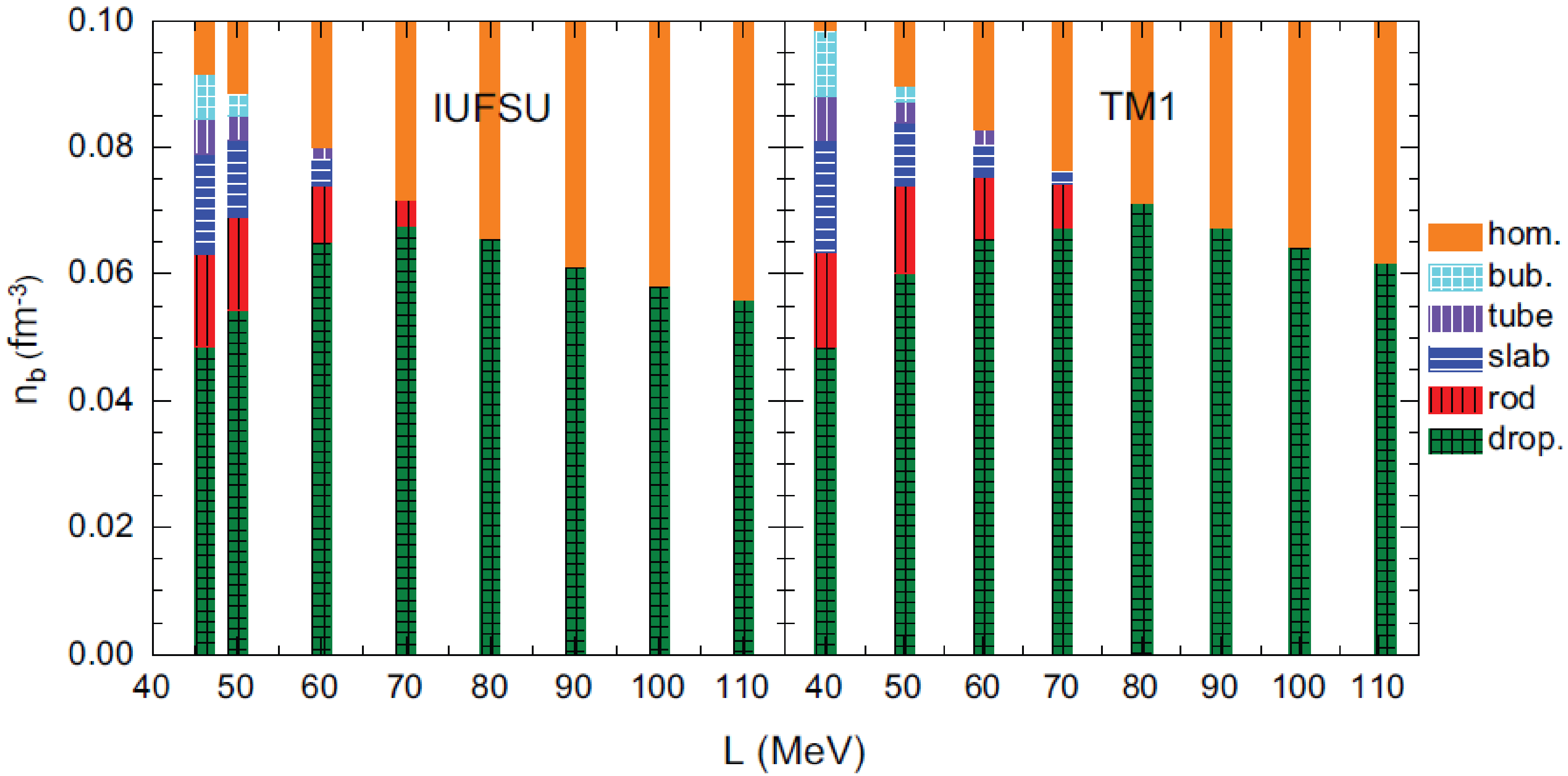

S. S. Bao, H. Shen, Phys. Rev. C 91, 015807 (2015)

smaller L corresponds to more pasta phases

smaller L corresponds to larger crust-core transition density

Summary

- Relativity is important at high density
- Several EOS tables are available
- Our EOS has been developed and checked
- Symmetry energy has important effects